# *Aspergillus fumigatus* can exhibit persistence to the fungicidal drug voriconazole

Jennifer Scott[1#], Clara Valero[1,2#], Álvaro Mato-López[3], Ian J. Donaldson[4], Alejandra Roldán[3], Harry Chown[1], Norman Van-Rhijn[1], Sara Gago[1], Takanori Furukawa[1], Alma Mogorovsky[5], Ronen Ben Ami[6], Paul Bowyer[1], Nir Osherov[5], Thierry Fontaine[7], Gustavo H. Goldman[2], Emilia Mellado[3], Michael Bromley[1] and Jorge Amich[1,3,*].

1. Manchester Fungal Infection Group (MFIG), Division of Evolution, Infection, and Genomics, Faculty of Biology, Medicine and Health, University of Manchester, United Kingdom.
2. Faculdade de Ciências Farmacêuticas de Ribeirão Preto, Universidade de São Paulo, Ribeirão Preto, Brazil.
3. Mycology Reference Laboratory (Laboratorio de Referencia e Investigación en Micología LRIM), National Centre for Microbiology, Instituto de Salud Carlos III (ISCIII), Majadahonda, 28222 Madrid, Spain.
4. Bioinformatics Core Facility, Faculty of Biology, Medicine and Health, University of Manchester, United Kingdom.
5. Department of Clinical Microbiology and Immunology, Sackler School of Medicine Ramat-Aviv, Tel-Aviv, Israel.
6. Sackler Faculty of Medicine, Tel Aviv University, Tel Aviv, Israel.
7. Institut Pasteur, Université de Paris, INRAE, USC2019, Unité Biologie et Pathogénicité Fongiques, F-75015, Paris, France.

# These authors contributed equally. They are ordered alphabetically

* Corresponding author: jamich@isciii.es

**ABSTRACT**

*Aspergillus fumigatus* is a filamentous fungus that can infect the lungs of patients with immunosuppression and/or underlying lung diseases. The mortality rates associated with chronic and invasive aspergillosis infections remain very high, despite availability of antifungal treatment. In the last decade, there has been a worrisome emergence and spread of resistance to the azole class of antifungals, which are the first line therapy for the treatment of *A. fumigatus* infections. The mortality caused by resistant isolates is even higher, and the management of these patients is complicated as the therapeutic options are severely reduced. Nevertheless, treatment failure is also common in patients infected with azole susceptible isolates, which can be due to several non-mutually exclusive reasons, such as poor drug absorption. In addition, the phenomena of tolerance or persistence, where susceptible pathogens have the ability to survive the action of an antimicrobial for extended periods of time, have been associated with treatment failure in bacterial infections, and their occurrence in fungal infections already proposed. Here, we investigated the *A. fumigatus* response to the azole voriconazole and demonstrate that certain isolates of this fungal pathogen can display persistence to this antifungal. A sub-population of the persister isolates can survive for extended periods and even grow at a slow rate in the presence of supra-MIC (minimum inhibitory concentration) of voriconazole. Persistence cannot be eradicated with adjuvant drugs or antifungal drug combinations and reduces the efficacy of treatment in a *Galleria mellonella* model of infection. Furthermore, persistence implies a distinct transcriptional profile, demonstrating that it is an active response to the drug. For all these reasons, we propose that azole persistence may be a relevant and underestimated factor that influences the outcome of infection in human aspergillosis.

## INTRODUCTION

*Aspergillus fumigatus* is the most prominent fungal pathogen of the human lung, being the major causative agent of a range of diseases collectively termed aspergillosis [1]. The incidence of fatal aspergillosis infections is on the rise due to the increase in the at-risk population [2, 3], including severe COVID-19 patients [4-6]. The mortality associated with *A. fumigatus* infections remains unacceptably high: 38% 5-year mortality rates for chronic pulmonary aspergillosis [7] and ranging from ~35% in early diagnosed and treated patients to nearly 100% if diagnosis is missed or delayed in invasive aspergillosis [8]. This is the highest mortality of all invasive fungal diseases [9]. This situation has become even more worrisome due to the emergence of clinical resistance to existing antifungals, which poses a serious threat to human health [10]. Azoles are currently the only FDA-approved class of mould-active agents that can be administrated orally and intravenously, and accordingly they are used for both the evidence-based treatment and prevention of aspergillosis diseases [11]. However, in the last decade the number of clinical *A. fumigatus* isolates that are resistant to triazole drugs has increased worldwide causing serious problems for clinical management, as the therapeutic options are reduced and the mortality rates caused by resistant isolates are higher [7, 12, 13]. Furthermore, both in clinical disease and in experimental animal models it has been observed that treatment failure is common even if the infecting fungal isolate is susceptible to the azole used for treatment [14, 15]. There are several possible explanations for treatment failure in these cases, including antifungal tolerance or persistence [16, 17].

In the last decade there has been a revolution in our understanding of how pathogenic microorganisms withstand the challenge of antimicrobial drugs. Classically, pathogens were described to be either susceptible or resistant to a certain drug. Antimicrobial resistance is due to a genetic feature in the microbe (intrinsic or acquired *via* mutations) that enables it to grow normally at high concentrations of the agent, above the Minimum Inhibitory Concentration (MIC) defined for the antimicrobial based on the clinical breakpoint. However, in recent years it has become obvious that microbes can withstand the action of drugs by at least three other mechanisms: tolerance, persistence, or heteroresistance. These three phenomena share the feature that they are not triggered by mutations in the microbe's DNA sequence, yet differ in other details. Drug tolerance has been defined as the ability of all cells of a genetically isogenic strain to survive, and even grow at slow rates, for extended periods in the presence of drug concentrations that are greater than the minimal inhibitory concentration (MIC). In persistence, only a small fraction of the isogenic population (usually <1% of the cells) survive, and grow at slow rates, for an extended period in the presence of supra-MIC concentrations of the drug [18, 19]. These two phenomena do not imply an increase in the MIC. Finally, heteroresistance is the transient capacity of a microbial subpopulation

to increase the MIC in the presence of the drug, due to adaptation, epigenetic modifications or reversible aneuploidy. All those phenomena have been implicated in treatment failure and relapse in bacterial infections [18, 20].

In fungi, tolerance has been often described as "trailing growth" and its relevance for infection has been mostly disregarded. However, a recent landmark study in *Candida albicans* has characterised tolerance as a distinct strain-specific feature and provided evidence for its relevance in persistent candidemia [17, 21]. In *Aspergillus*, trailing growth is known to be prominent in the presence of caspofungin [22, 23] apparently due to single strain heterogeneity [24]. Moreover, at higher concentrations of this drug some isolates can resume normal growth, an effect known as "Eagle" or paradoxical effect (see review [25] for more information), which we have recently demonstrated as a tolerance phenotype [26]. The possible relevance of the paradoxical effect in clinical practice is still under debate, but there is evidence suggesting that it might be important [27], and concern has been raised by some clinicians [28]. Remarkably, it seems that the phenomenon of tolerance in fungi is seen with static drugs, e.g. azoles for *C. albicans* and echinocandins for *A. fumigatus*. However, the possibility that *A. fumigatus* can display tolerance or persistence to azole antifungals had not been previously investigated. Interestingly, in contrast to *C. albicans* and *Cryptococcus neoformans*, azoles have been shown to have fungicidal activity against *A. fumigatus* [29-31], which implies that the underlying mechanisms are likely different. Whilst these phenomena have so far only been investigated in bacteria or yeasts, the approaches to detect and investigate azole tolerance or persistence need to be tailored to filamentous fungi, like *A. fumigatus*, as these organisms form multicellular hyphae. Using various complementary approaches, we show that small subpopulations of certain *A. fumigatus* isolates can survive and even grow at slow rates at supra-MIC concentrations of the fungicidal drug voriconazole.

## RESULTS

### Some *Aspergillus fumigatus* isolates show persistence to voriconazole

To determine whether *A. fumigatus* can display tolerance or persistence to voriconazole, we examined a collection of isolates consisting of 9 environmental, 10 clinical (gift from Prof Paul Dyer, collection PD-47-XX, here shortened as PD-XX), 5 common laboratory strains and one resistant control (RC) harbouring the TR34/L98H mutations in the *cyp51A* locus (Table S1) using disc diffusion assays. We evenly spread $4\times10^4$ conidia of the isolates on RPMI agar plates, placed a 6 mm disc in the centre, containing 10 µL of voriconazole (0.8 mg/mL), and incubated them for 5 days. We observed variability in the sizes of the inhibition halos, reflecting differences in susceptibility of the isolates (Figs. 1A and S1). As expected, the RC strain did not show a proper inhibition halo (Figs. 1A

and S1). In contrast, 15 of the 20 isolates showed a clear and well-defined inhibition zone. Interestingly, we found that 5 isolates were able to form colonies within the halo of inhibition, and 4 in 5 of these isolates (PD-9, PD-104, PD-254 and PD-266, Fig. S1) formed only a few small colonies, which might be indicative that a few conidia are able to germinate and grow at a slow rate in the presence of a supra-MIC concentration of voriconazole (Fig. 1A and S1). The other isolate (PD-256) did not show any inhibition halo, suggesting that it is a resistant isolate.

We then assessed the MICs of the original isolates and their derived colonies of the halo (CoHs). A complication of working with a filamentous fungus is that the CoHs need to be grown on a new plate in order to harvest spores (conidia) to be used for MIC determination. We therefore decided to assay two different conidia-harvesting conditions to distinguish the different phenotypes: re-growing the CoHs on solid RPMI in the absence or in the presence of a low concentration of voriconazole (0.12 µg/mL). It would be expected that for conidia grown in the presence of the drug, both resistance and heteroresistance are detected as an increment in the isolate's MIC. In contrast, for conidia grown in the absence of the drug, the reversible increase in MIC that is characteristic of heteroresistance would be lost, whilst a stable genetic-based increment in MIC that defines resistance would be maintained. Finally, persistence should not cause a change of the isolate's MIC independently of the presence of the drug in the conidia-harvesting medium. Using conidia obtained from both conditions, absence and presence of voriconazole, we found that the original isolate did not show an inhibition halo (PD-256, Fig 1A and S1) had a very high MIC (>8 µg/mL), demonstrating that it is a resistant isolate (Table 1). CoHs formed by PD-254 and PD-266, which upon re-inoculation did not show an inhibition halo (Fig S1), showed an increased MIC compared to the parental isolate (Table 1). The colony picked from PD-254 showed increased MIC when re-grown on both media with and without voriconazole, suggesting that the CoH may have acquired a mutation that confers a stable resistance phenotype. In contrast, PD-266, which already had an elevated MIC, only showed an increased MIC when re-grown on medium containing voriconazole, suggesting that this strain may be heteroresistant. Finally, CoHs from isolates PD-9 and PD-104 showed the same MICs as their original isolates after a passage in the absence or presence of voriconazole (Table 1). This suggests that they are not resistant or heteroresistant derivatives of the original isolates. Indeed, repetition of the disc assay with the original isolates and with CoH re-grown in the presence of voriconazole, showed a similar level of colony appearance in the original strains and their derived CoHs for PD-9 and PD-104 (whereas it grew to the edge of the disc for PD-266, reflecting again a transient increase in its MIC) (Fig S1). Interestingly, all isolates showed a small increase (one dilution) in MIC when re-grown in the presence of drug (Table 1). This may be due to the development of conidia adapted to

the growing environment in preparation for the subsequent germination, an effect recently described in *Aspergillus spp* [32].

| | Voriconazole MIC (µg/mL) | | | | |
|---|---|---|---|---|---|
| **Isolate** | **original** | **Original (grown on Drug)** | **CoH (- Drug)** | **CoH (grown on Drug)** | **Classification of CoH** |
| ATCC | 1 | 2 | | | Susceptible |
| PD-9 | 0.5 | 1 | 0.5 | 1 | Persister |
| PD-104 | 1 | 2 | 1 | 2 | Persister |
| PD-254 | 2 | 2 | >8 | >8 | Resistant |
| PD-256 | >8 | >8 | >8 | >8 | Resistant |
| PD-266 | 4 | 8 | 4 | >8 | Heteroresistant |

**Table 1**. Voriconazole MIC for original isolates and their derived COHs

In bacteria, persister and tolerant cells are often dormant and do not grow [19]. To investigate this in *A. fumigatus* in more detail, we followed a protocol to detect tolerance/persistence in bacteria in which the disc containing the drug, after a period of incubation, is switched with another one containing fresh media [33]. The rationale is to detect surviving cells that have remained dormant and resume growth after the drug is withdrawn. After initial growth we substituted the disc with voriconazole for a new one containing *Aspergillus* Minimal Media (AMM). Interestingly, after the disc switch colonies were observed in the halos for several isolates (PD-7, -8, -50, -154, -249, and -264, Fig. S2), suggesting that these may be low level persister isolates. Nevertheless, three isolates, PD-9, -104 and -259, were able to form colonies before the disc switch, and of these three, only PD-9 and PD-104 grew even more colonies after disc switch (Fig. S2). Therefore, the isolates PD-9 and PD-104 were able to survive and grow at slower rates in the presence of supra-MIC concentrations of voriconazole, a phenomenon that complies with the definition of persistence.

To further characterize persistence in *A. fumigatus*, we performed MIC assays with selected strains and checked microscopic growth of persister and non-persister isolates at supra-MIC concentrations. We found that 72 hours after inoculation the non-persister strains ATCC46645 and PD-60 displayed microscopic growth only at the MIC concentration, and no growth at all at higher concentrations (Figs. 1B and S3). In contrast, the persister isolates PD-9 and -104 showed noticeable microscopic growth at 2X, and even at 3X MIC germinated conidia could be detected (Fig. 1B and S3). While the level of growth was variable among independent experiments, the difference between persister and non-persister isolates was consistently observed (Fig. 1B and S3). In addition, we plated the entire content of the wells containing the highest concentrations of voriconazole (8 µg/mL) and found that 48 h after inoculation the non-persister strains were nearly all killed (only ~0.07% of the conidia survived) whilst in the persister strains a significantly higher ratio of conidia survived (0.39% of PD-9 $p$=0.002 and 0.18% of PD-104 $p$=0.0331, Fig. 1C). Therefore, a subpopulation of the *A. fumigatus*

persister isolates can survive for long periods in the presence of high concentrations of voriconazole and even grow at a slow rate, which seem to be inversely correlated with the concentration of drug.

In bacteria, a combination of MIC and speed of killing is the best approach to reveal and differentiate tolerance and persistence [18]. Therefore, we investigated the dynamics of cell death caused by voriconazole for persister and non-persister isolates. Conidia from two susceptible (ATCC46645 and PD-60), two persister (PD-9 and PD-104) and the putative heteroresistant (PD-266) strains were incubated for 4 days in liquid RPMI in the presence of 4 µg/mL of voriconazole and aliquots of the culture plated (after PBS washing to remove the drug) on PDA rich media every 24 hours (Fig. 1D). We found that for all strains the number of viable conidia dramatically declined after 24 hours of incubation, reflecting a strong fungicidal action of voriconazole, even against an isolate with high MIC. Interestingly, whilst the susceptible isolates were completely killed within 48-72 hours, a considerable number of conidia from the persister strains maintained viability for an extended period of time (~0.748% for PD-9, ~0.136% for PD-9 at 48 h and ~0.52% for PD-9, ~0.128% for PD-9 at 72 h, Fig. 1D), resulting in the characteristic biphasic killing curve that is the hallmark of persistence [19]. The isolate PD-266 showed visible growth from 72h, which agrees with its proposed heteroresistant phenotype, and saturated the plate at the last time-point. To investigate the survival of the isolates at the single cell (conidial) level, we incubated the two persister and one susceptible strains in liquid RPMI in the presence of 32 µg/mL voriconazole for 48 hours, and replaced it with fresh drug free medium. We observed that during the first 24 hours of incubation after drug withdrawal there was no growth for any of the isolates, but subsequently the persister strains were able to resume growth (Videos S1 and S2) whilst the susceptible strain was not (Video S3). Hence, persister strains indeed can survive for extended periods in the presence of high concentrations of voriconazole and resume growth when the drug is withdrawn.

To check if the observed phenomena could be explained by mutations in the target gene *cyp51A*, we sequenced the promoter and ORF of the encoding gene in the persister isolates PD-9 and PD-104 and the non-persister strain PD-60. In all strains we found that *cyp51A* was completely wild-type (not shown), denying an implication of target enzyme mutations in the phenomenon persistence. We also sequenced the sterol-sensing domain of *hmg1*, as it has been proposed that mutations in this gene may be a precursor step for the development of azole resistance [34, 35], and in bacteria persistence has been shown to correlate with the evolution of resistance [36, 37]. However, we found again that all strains harboured a completely wild-type sequence (not shown), suggesting that *hmg1* is not related with voriconazole persistence.

In conclusion, we have observed that certain *A. fumigatus* isolates can survive and grow at slow rates for extended periods of time in the presence of supra-MIC concentrations of voriconazole, therefore, these isolates display persistence to voriconazole.

**_Aspergillus fumigatus_ persistence is maintained in the hyphal transition and seems to be medium dependent.**

*A. fumigatus* undergoes morphological changes during its development, shifting from resting conidia to swollen conidia (~4-5 h), then to germlings (~8 h) and finally forming hyphae (~16 h). As the cellular metabolic status is different at each developmental stage [38], we speculated that it might influence the capacity of the fungus to deploy persistence in the presence of voriconazole. To investigate this possibility, we incubated the RPMI plates inoculated with the fungus for 8 or 16 hours before adding the drug to the disc. We found that the persister strains PD-9 and PD-104 were also able to form colonies in the halo when drug was added 8 hours after the beginning of incubation (Fig. 2A), suggesting that persistence is not determined by the developmental stage. We could not draw definitive conclusions for the 16 hours grown hyphae, as the background growth was too dense to undoubtedly differentiate specific persister colonies (Fig. 2A). Nevertheless, we could clearly detect a growing colony in the voriconazole halo for the strain PD-104 (Fig. 2A), proving that at least this strain can display persister growth when short hyphae are challenged with the drug. Interestingly, it has previously been reported that morphological status alters *A. fumigatus* susceptibility profiles against various drugs including voriconazole [39], which supports the notion that persistence is a different phenomenon, triggered by distinct mechanisms, and independent of MIC.

To determine if persistence is influenced by the growth medium, we performed a voriconazole disc diffusion assay with the PD-104 isolate and the wild-type control ATCC46645 on PDA rich media or AMM. The PD-104 strain showed persister growth on both media, and it seemed to be able to form a higher number of COHs on PDA rich media (Fig. 2B). The ATCC46645 wild-type strain did not show persistence on AMM, but surprisingly it did form colonies in the halo on PDA media (Fig. 2B). To investigate this in more detail we repeated the disc assay using two different rich media, PDA and Sabouraud, with more strains, CEA10, PD-9, and PD-60 (Fig. 2C) and found that all strains were able to form colonies in the halos. The MICs of the isolates, measured by broth dilution assay, were equal on Sabouraud and RPMI (Fig. 2D), indicating that the effect of the drug is not reduced in rich medium. Therefore, the ability of *A. fumigatus* to display persistence seems to be medium dependent, suggesting that a rich nutrient environment favours survival at supra-MIC concentrations. This is supported by a recent study that showed that a rich metabolic environment can promote azole tolerance in *Saccharomyces cerevisiae* [40]. Nevertheless, it should also be

considered that voriconazole diffusion may be affected in solid rich media, which could be confounding this observation.

**_Aspergillus fumigatus_ persistence to voriconazole is independent of stress and cannot be inhibited with adjuvant or antifungal drugs.**

Changing environmental conditions activate signalling cascades that trigger transcriptional adaptation and cell wall alterations [41-44]. Therefore, we reasoned that the capacity of certain isolates to survive and grow in supra-MIC concentrations of voriconazole might be influenced by environmental stressors. Indeed, in *C. albicans* mutants and inhibitors of stress response pathways eliminate tolerance [45]. To investigate this possibility, we analysed voriconazole persistence of PD-104 in the presence of hypoxic (1% $O_2$), oxidative (0.01% $H_2O_2$), osmotic (150 mM NaCl), membrane (0.05% SDS) and cell wall (10 µg/mL CalcoFluor White) stress. Surprisingly, in contrast to *C. albicans* [21], we found that most environmental conditions did not influence persistence in *A. fumigatus* (Fig 3A). This suggests that the underlying mechanism(s) of persistence in *A. fumigatus* are likely different from the previously proposed mechanisms of tolerance in *C. albicans*. The only condition that influenced *A. fumigatus* persistence was hypoxia, which could prevent growth in the halo (Fig. 3A). As we had observed above that persistence was influenced by the growth medium, we wondered if hypoxia could prevent persistence also on rich medium. As shown in Figs 2B and 2C, all isolates were able to grow colonies in the halo when grown on the rich medium YAG on normoxia (Fig. 3B). However, persistence was eliminated under hypoxia for all strains, except for PD-104, for which it was reduced but apparently not completely eradicated. Therefore, it seems that hypoxia reduces persistence, but the nutritional composition of the medium also influences its impact on the phenomenon.

In *C. albicans*, fluconazole tolerance (but not resistance) can be prevented with the use of adjuvant drugs that block general stress signalling pathways [21]. To further investigate if the underlying mechanism of persistence may be different in *A. fumigatus*, we tested the effect of various drug adjuvants that were previously shown to eliminate tolerance in *C. albicans* [21]: geldanamycin (0.8 µg/mL), an inhibitor of heat shock protein (Hsp90) [46, 47], FK506 (4 ng/mL), an inhibitor of calcineurin [48], H-89 (4 µg/mL), an inhibitor of the cAMP-dependent protein kinase (PKA) [49], rapamycin (6.25 µg/mL), an inhibitor of the mammalian target of rapamycin (mTOR) [50], and tunicamycin (10 µg/mL), an inducer of the unfolded protein response pathway [51]. In contrast to *C. albicans*, the use of adjuvant drugs did not prevent persistence of *A. fumigatus* isolates (Fig. 3C). We also tested lovastatin (8 µg/mL) and simvastatin (2 µg/mL), as statins inhibit 3-hydroxy-3-methylglutaryl-coenzyme A (HmgA) [52], an enzyme in the same metabolic pathway as the target of azoles, and these two were previously shown to have antifungal activity against *Aspergillus spp* [53].

However, statins were also not able to prevent persister growth (Fig. 3B). Finally, as efflux of antifungals has been proposed to play a role in *C. albicans* tolerance [45], we tested if the efflux inhibitors milbemycin A oxim (8 µg/mL) [54] or clorgyline (63.5 µg/mL) [55] can prevent *A. fumigatus* persistence. These compounds seemed to be able to diminish the persister capacity of the strains, as only one CoH per plate could be detected, and these colonies were exactly at the edge of the halo (Fig. 3C). In conclusion, adjuvant drugs cannot prevent *A. fumigatus* persistence to voriconazole, and efflux inhibitors may affect this process and deserve further study.

Next, we evaluated if persistence can be eradicated using combinatorial treatment with the other classes of antifungal drugs in clinical use. However, neither amphotericin-B (1 µg/mL) nor caspofungin (0.5 µg/mL) could prevent persistence (Fig. 3D). Interestingly, these antifungal drugs could also not impede growth in the halo of the presumed heteroresistant strain PD-266 (Fig. 3D). Therefore, it seems that combinatorial treatment with other antifungals cannot prevent persistence in *A. fumigatus*.

**The phenomenon of persistence can be observed with other azole drugs**.

To check if *A. fumigatus* can display persistence in the presence of other azoles, we firstly employed the disc diffusion assay adding 10 µL of a 3.2 mg/mL itraconazole solution. We found that the isolates PD-104 and PD-266 were able to form colonies in the halo (Fig. S4). Upon re-inoculation of a CoH (re-grown in itraconazole containing media), the isolate PD-104 showed an inhibition halo of the same size and displayed similar level of CoH appearance, whereas the PD-266 isolate was able to grow on the whole plate and did not show any inhibition halo. Therefore, this suggests that, as observed with voriconazole, the isolate PD-104 is persistent and the isolate PD-266 is heteroresistant to itraconazole. We then performed a broth dilution assay with our four well-characterised isolates (non-persisters ATCC46645 and PD-60 and persisters PD-9 and PD-104) to calculate the MIC for itraconazole and isavuconazole, and looked under the microscope at supra-MIC concentrations (Fig. S5A and S5B). We found that the isolates PD-9 and PD-104 showed slight growth at 2X MIC, whilst ATCC46645 and PD-60 did not (Fig. S5B). Moreover, we inoculated the entire content of wells containing the highest concentration of the drugs (8 µg/mL) on PDA plates, and found that a detectable number of conidia from the isolates PD-9 and PD-104 remained viable after 48 hours of incubation in the presence of the azoles. Hence, even if more experiments need to be done for a detailed characterization of persistence to these azoles, these results suggest that the same isolates that are persisters to voriconazole could also display persistence to itraconazole and isavuconazole.

**The transcriptome of persister growth suggest that Galactosaminogalactan and high expression of sterol biosynthetic genes may be relevant to establish persistence.**

To better understand the heterogeneous nature of persistence, we compared the transcriptome of PD-104 grown under conditions favouring persistence (above MIC), sub-MIC and in the absence of drug. We inoculated the spores on top of a nylon membrane placed on an RPMI solid plate. We put the disc with voriconazole (0.8 mg/mL) on the membrane and incubated for 5 days at 37°C. Standard halos of inhibition formed on the membrane, and persister colonies appeared for the PD-104 strain, but not for the A1160 strain (Fig. S6A). We harvested mycelium (avoiding conidia as much as possible) from plates without a voriconazole disc (No Drug), from the area equidistant from the border of the plate and the inhibition halo (Low Drug) and the colonies in the halo (Persistence) (Fig. 4A). We had to combine persister colonies from 20 plates per replicate in order to obtain sufficient material for RNA extraction. Additionally, we harvested mycelia from A1160 with No Drug and Low Drug under the same conditions. We performed RNA-seq and compared the transcriptomes of the following conditions (i) A1160 Low Drug VS No Drug, (ii) PD-104 Low Drug VS No Drug, (iii) PD-104 Persistence VS No drug and (iv) PD-104 Persistence VS Low Drug. We defined differentially expressed genes (DEG) as those with a log2FoldChange >1 or <-1 and a false discovery rate (FDR) <0.05.

In A1160, we detected 62 genes upregulated in the presence of low voriconazole concentrations and only 4 that were downregulated (Fig. 4A and Dataset S1). Such a low number of DEGs may be due to the relatively low concentration of voriconazole in the harvested area. Nevertheless, among the upregulated genes we found 10 related to sterol biosynthesis (Dataset S1), including *cyp51A* and *cyp51B*, the expression of which have been reported to increase upon azole challenge [56, 57]. Surprisingly, only 21 of the 62 upregulated genes overlapped with our previously published dataset, in which 1492 genes were upregulated upon challenge of A1160 with itraconazole [58]. This striking difference may be due to the different drug employed, the different concentrations assayed and/or the use of solid medium. Interestingly, these 41 DEGs that are specific to this analysis (which can be found in Dataset S1) contain *cyp51A*, *cyp51B* and various other genes of the sterol pathway.

For PD-104, the Low Drug VS No Drug comparison retrieved 32 genes upregulated and only 1 downregulated (Fig.5 and Dataset S2). Within the upregulated genes we again found 8 genes related with sterol biosynthesis, including *cyp51A*. In addition, 9 genes did not overlap with the comparison of A1160 (Fig. 4A and Dataset S2). These differences with A1160 may point to potential strain differences in response to voriconazole. In the Persister VS No Drug comparison there were 802 upregulated and 249 downregulated genes and in the Persister VS Low Drug 646 upregulated and 187 downregulated genes (Fig. 4A and Dataset S2). When comparing those three analyses, only 53 genes were exclusively upregulated and 39 downregulated in Persister VS Low Drug (detected using

BioVenn [59]), suggesting that they may be important to establish the persister phenotype and not only as a response to the drug (Fig. 4A and Dataset S2). We performed Gene Ontology (GO) enrichment analyses (on FungiDataBase [60]) for these 53 DEGs, which retrieved a number of biological processes and molecular functions for up- and downregulated genes. It is important to note that the FDR did not reach significance for any of them, which is possibly due to the low number of genes included in the analysis. However, we believe this analysis provided interesting clues and can help to direct future research. For the up-regulated genes, the strongest enrichment was for the biological processes galactose and aldehyde metabolisms (Fig. 4B) and the molecular function oxidoreductase activity (Table S2). Interestingly, galactose metabolism was found to be the most upregulated function in *Staphylococcus aureus* persisters, although the reason has not been elucidated yet [61]. For the downregulated genes, there was an enrichment of biological processes related with development and cell cycle (Table S2), possibly reflecting the reduced growth rate in this condition.

Interestingly, a significant number of the detected differentially expressed mRNAs in PD-104 were not assigned to any gene of the A1163 genome reference used for the mapping of the reads. In detail, 80 of the upregulated (including 4 of the 20 most upregulated) and 29 of the downregulated for the Persister VS no Drug comparison and 55 upregulated (including 5 of the 10 most upregulated) and 14 downregulated for the Persister VS no Low comparison seem to have no orthologue in A1163 (Dataset S2). This points to the requirement of a high number (~10% of the DEG) of strain specific genes to facilitate for persister growth. Therefore, we re-annealed the sequenced mRNAs from the PD-104 isolate to the newly generated *A. fumigatus* pangenome [62] and performed the comparisons again (Dataset S3). In this analysis, the Persister VS no Drug comparison retrieved 811 genes up- and 260 downregulated, and the Persister VS Low Drug comparison 659 up- and 193 downregulated (Fig. 4A and Dataset S3). The ratio of identified genes greatly improved, as only ≤1.8% of the DEGs could not be assigned to an ID. Yet, the most upregulated gene in the Persister VS Low Drug comparison was an unidentified gene and many of the newly identified genes encode uncharacterised hypothetical proteins, which reflects our ignorance of *A. fumigatus* biology and thus how difficult it is unravelling underlying mechanisms in this pathogen. GO enrichment analysis of all DEGs showed that secondary metabolism, ergosterol metabolism and transport were key upregulated biological processes (Fig. 4C) and oxidoreductase, catalysis and transmembrane transport important molecular functions (Table S3), all of which suggests an active metabolic response in persister conditions. As observed above (Table S2), downregulated biological processes reflected a downregulation of developmental processes (Table S3). Comparison of the DEGs present in all three comparisons revealed that 64 genes were

exclusively up- and 46 downregulated in Persister VS Low Drug (detected using BioVenn [59]), suggesting that they may be specifically important for persistence (Fig. 4A and Dataset S3). GO enrichment analysis of those genes revealed galactosaminogalactan (GAG) biosynthesis as the most significant upregulated biological process (Fig. 4D and Table S4), providing a plausible explanation for the upregulation of galactose metabolism observed before, and suggesting that this exopolysaccharide may be relevant for persistence in *A. fumigatus*. Next, we performed a protein functional association analysis using the STRING database and platform [63] to investigate if these 64 upregulated genes are functionally correlated. Sixty-one of these genes could be matched to proteins in the database, showing a significant ($p$=1.84e-08) interaction network, including a node of 17 proteins related with metabolism (Fig S6B and Table S5). This suggests that a distinct metabolic response occurs during persister growth.

Bacterial persistence has been proposed to be a sub-population event due to stochastic high expression of relevant genes [64, 65]. Accordingly, we reasoned that those genes that are upregulated in Low Drug VS No Drug and Persister VS No Drug comparisons, but also in Persister VS Low Drug might reveal those genes that are important to adapt to presence of the drug, but also that can create persistence with higher levels of expression. We identified 18 genes that appeared as upregulated in all three comparisons (Fig. 4A and Table 2), indicating that they have higher levels of expression in persistence VS normal response to the drug. GO enrichment analysis revealed sterol metabolism as the most significantly upregulated biological process (Fig. 4E and Table S7). Indeed, those few genes had a very significant enrichment in the KEGG pathway “steroid biosynthesis” (Table 2), suggesting that high expression of genes in the sterol biosynthetic route (including *cyp51A*) may enable the sub-population of persisters to survive and grow in supra-MIC concentrations. Additionally, these highly expressed genes were enriched in KEGG pathways related with cytochrome P450 dependent drug metabolism (Table 2), which may indicate that detoxification of azoles is also important for persistence. Finally, expression of the *cdr1B* transporter (AFUA_1G14330), known to be associated with azole resistance [66], was also detected to be higher in persistence (Table 2). This suggests that a higher capacity to efflux azoles may also be important for the persister phenotype. Finally, we performed a protein functional association analysis with these 18 genes using the STRING database and platform [63] to search for functional correlations. All 18 genes were matched to proteins and a significant interaction ($p$<1.0e-16) was found, involving a highly interactive nodule of 6 proteins related with steroid biosynthesis (Fig. S6C and Table S6), suggesting again that a high production of ergosterol is important for persistence.

| Gene ID | Product description |
|---|---|
| AFUA_1G03200 | Putative major facilitator superfamily (MFS) transporter |
| AFUA_4G06890 | 14-alpha sterol demethylase Cyp51A |
| AFUA_2G00320 | putative sterol delta 5,6-desaturase |
| AFUA_3G00810 | Putative cholestenol delta-isomerase |
| AFUA_1G03150 | C-14 sterol reductase, putative |
| AFUA_8G02440 | C-4 methyl sterol oxidase, putative |
| AFUA_6G14140 | Has domain(s) with predicted role in response to stress and integral component of membrane localization |
| AFUA_3G00150 | Has domain(s) with predicted oxidoreductase activity and role in metabolic process |
| AFUA_4G01440 | Predicted glutathione S transferase |
| AFUA_4G04820 | C-4 methyl sterol oxidase Erg25, putative |
| AFUA_5G00840 | Ortholog of A. nidulans FGSC A4 : AN5639, AN2587, AN9444, AN7395, |
| AFUA_2G15130 | ABC multidrug transporter A-2, putative |
| AFUA_5G03290 | Ortholog of A. nidulans FGSC A4 : AN8197, A |
| AFUA_3G02520 | Has domain(s) with predicted role in transmembrane transport and integral component of membrane localization |
| AFUA_7G04740 | Ortholog of A. fumigatus Af293 : Afu1g01960, Afu3g01040, Afu3g03315, Afu7g01960, Afu8g05750, Afu5g00135, Afu7g06526 |
| AFUA_2G01890 | Ortholog(s) have 2-octoprenyl-3-methyl-6-methoxy-1,4-benzoquinone hydroxylase activity, |
| AFUA_1G14330 | Azole transporter |
| AFUA_8G00710 | Has domain(s) with predicted role in defense response, negative regulation of growth |

| KEGG Pathway ID | Name | P-value | Benjamini |
|---|---|---|---|
| ec00100__PK__KEGG | Steroid biosynthesis | 2,31E-08 | 1,18E-06 |
| ec00980__PK__KEGG | Metabolism of xenobiotics by cytochrome P450 | 0.002873 | 0.073261 |
| ec00982__PK__KEGG | Drug metabolism - cytochrome P450 | 0.004423 | 0.075206 |

**Table 2.** List of genes that are more upregulated in Persister growth. KEGG pathway enrichment analysis of those genes

**Galactosaminogalactan potentiates persistence of PD-104.**

Our transcriptome analysis detected a significantly higher expression of two GAG biosynthetic genes (*sph3*, AFUA_3G07900 and *uge3*, AFUA_3G07910) in persister growth (Dataset S3). Manual inspection of the GAG biosynthetic genes [67, 68] revealed that another gene (*agd3*, AFUA_3G07870) might also be upregulated (FC= 1.01), but although the *p*-value was significant (*p*= 0.0179), the FDR rate was above threshold (FDR=0.1167) (Dataset S3). This prompted us to investigate if a higher amount of GAG could create and/or potentiate persistence in *A. fumigatus*. To this aim, we performed broth dilution assays in which we inoculated each isolate (ATCC, PD-9,

PD-60 and PD-104) in two different lines and added purified GAG at a concentration of 100 µg/mL to one of them. Comparison of the MIC with and without GAG demonstrated that this polysaccharide did not affect the resistance profile of the isolates (Fig. 5A). After reading the MIC at 48 hours, we added 10 µg/mL of the dye calcofluor white (CFW) to the wells and imaged the entire well (87 photos using a 20X objective) at the blue emission channel. Images were merged (Fig. 5B) and the number of germinated conidia/short hyphae in the whole well calculated as explained in materials and methods (Fig. 5B). By these means we could calculate that ~2% of the PD-9 spore population and ~1% of the PD-104 conidia were able to germinate at 2X MIC, and ~0.35% for both isolates in 3X MIC. Interestingly, addition of GAG enhanced the number of persisters in PD-104 (from 1.09% to 2.80%, $p$=0.0267 at 2X MIC and from 0.41% to 0.75% $p$=0.038) but not in PD-9 (Fig. 5B). Next, we inoculated the four isolates in duplicated lines of 96-well plates containing a high concentration of voriconazole (4 µg/mL) in all wells, and added GAG to one line of each isolate. The entire contents of wells were plated 48 hours after inoculation on PDA rich plates to count the number of viable CFUs. As observed before (Fig. 1C), we found that the persister isolates (PD-9 and PD-104) maintained viability of a significant number of conidia for an extended period of time (Fig. 5C). Interestingly, GAG addition seemed to slightly increase the number of grown CFUs for all isolates, although this increment was only significant for the PD-104 isolate (PD-104 VS PD-104+GAG $p$=0.0437).

These results suggest that a high level of GAG can potentiate persistence in some, but apparently not all, isolates. Future investigations will aim to understand the underlying mechanism and to determine why GAG addition is isolate-specific.

**Persistence can be detected in diverse *A. fumigatus* collections of isolates**

To corroborate that certain *A. fumigatus* isolates display persistence to voriconazole, we decided to screen two independent collection of isolates. Initially, we tested an environmental library of isolates collected in the area of Manchester, UK [69]. We screened all 157 isolates for growth under the microscope after 72 hours incubation in the presence of a high concentration of voriconazole (8 µg/mL). We found that 34 isolates were able to show a limited degree of growth, suggesting that they might be persisters (Table S8). Next, we employed disc diffusion assays with 0.8 mg/mL voriconazole and observed that 15 out of the 34 isolates were able to form colonies in the halo (Table S8). Broth dilution assay with the original isolates and the CoHs revealed that 10 of those isolates did not have increased MICs, indicating that they were persister strains (Table S8). Therefore, at least ~6% of this collection was persister to voriconazole. We further evaluated a collection of 17 azole-susceptible clinical isolates obtained from TAU medical centre (Table S8), which were prior shown not to have any mutation in the *cyp51A* gene promoter or ORF, using the disc diffusion assay. We found that 6 out of 17 (35%) isolates were able to grow small colonies in the

inhibition halo (Fig. S7A). Colonies picked from within the halo formed upon re-inoculation similar size halos, indicating that the MIC had not increased, and grew a similar number of CoHs, suggesting that the isolates are persisters.

Therefore, evaluation of independent collection of isolates seem to always retrieve a significant number of persister strains, demonstrating that this is quite a common phenomenon.

**Persistence is not a lineage specific trait.**

Recent studies suggest that the tandem repeats (TRs) in the promoter region of *cyp51A*, which cause high levels of antifungal resistance, possibly have evolved in the environment, due to the use of demethylase inhibitors (azoles) in the fields [70]. Interestingly, the isolates with the $TR_{34}$/L98H polymorphism have been found to be closely related [62, 70], which suggest that this mechanisms has evolved in a distinct lineage of the species. To investigate if the phenomenon of persistence could also be lineage specific, we sequenced the genome of 23 of our isolates, 12 persisters and 11 non-persisters (Table S8) and integrated their genome into a recently published phylogenetic analysis [62]. We found that both persister and non-persister isolates scattered through the entire tree, demonstrating that persistence is not a trait of a specific lineage of *A. fumigatus* (Fig. 6). In addition, it is noteworthy that some persister and non-persister isolates seem to be genetically very similar, as they are close in the tree (JA12-JA14-JA7-JA8 and also JA1-JA2, Fig. 6). This suggests that the genetic features that enable persistence are modest and/or that non-genomic features, as the transcriptional response, are important for isolate specificity.

**Persister isolates are less efficiently eliminated with a voriconazole treatment in a *Galleria mellonella* infection model.**

To evaluate if persistence may be relevant during antifungal treatment, we employed the *Galleria mellonella* mini-host model of infection. This model has been successfully used to investigate the efficiency of azole treatment against *A. fumigatus* [71, 72]. In addition, a recent study has characterised the pharmacokinetics of voriconazole in infected larvae, which helped us select the optimal dose to reach a high concentration of the drug in the haemolymph, but that is nearly completely removed in 24 hours [73].

Initially, we performed a survival experiment with all four strains to investigate if they could have different virulence potential. We infected larvae with $10^4$ conidia of non-persister (ATCC46645 or PD-60) or persister (PD-9 or PD-104) isolates and followed mortality for 10 days. At the isolates killed larvae at a similar rate (Fig. 7A), demonstrating that they are similarly virulent. Therefore, we aimed to use this model to investigate if persistence could potentially cause treatment failure. We reasoned that a voriconazole treatment should very efficiently eradicate susceptible, non-persister

strains, but it may not be able to eliminate persister strains with the same efficiency. We infected larvae with $10^4$ conidia of non-persister (ATCC46645 or PD-60) or persister (PD-9 or PD-104) isolates, administered one dose of 8 μg/larva voriconazole or PBS at the time of infection, and measured fungal burden 72 hours after infection. As expected, voriconazole treatment was efficient and dramatically decreased fungal burden for all isolates (Fig. 7B). Interestingly, the mean reduction in burden was bigger for non-persisters isolates (55.0X for ATCC46445 and 47.5X for PD-60, Fig. 6B) than for the persisters (9.8X for PD-9 and 15.8X for PD-104, Fig. 6B). Indeed, whilst some larvae from all groups had been completely cured with the treatment, three larvae from both PD-9 and PD-104 infected groups still had a considerable fungal burden, whilst only one larva from ATCC46645 or PD-60 had similar levels (Fig. 7B). Therefore, these results suggest that persister strains are less efficiently eliminated by a voriconazole treatment than non-persister isolates *in vivo*.

## DISCUSSION

The phenomenon of persistence to antimicrobials was first observed in bacteria 80 years ago [74, 75]. In the last decade, intensive research has permitted unravelling various underlying mechanisms in diverse bacteria, and it has become clear that persistence can cause treatment failure and lead to the development of resistance [76, 77]. However, our insight into antifungal persistence and tolerance in fungal pathogens is still in its infancy.

We have recently shown that all conidia in a tolerant *A. fumigatus* isolate are able to grow at high concentrations of caspofungin [26]. In *C. albicans*, tolerance to fluconazole was described to be a sub-population effect, but the ratio of tolerant cells was reported to be elevated [21]. In both cases, tolerance was observed in response to static drugs, so it seems that the phenomenon of tolerance in fungi associates with fungistatic drugs. In *C. albicans*, the formation of amphotericin-B (AmB) persister cells has been described [78]. Of note, this phenomenon has only been described within biofilms, and cannot be found in planktonic cells [79], possibly due to the physical protection conferred by the biofilm, which may be relevant for the capacity of these cells to survive in the presence of AmB. Indeed, in *A. fumigatus* it was shown that the hypoxic microenvironment developed in biofilms led to reduced metabolic activity in the basal biofilm level leading to the formation of cells that can survive the antifungal challenge, and serve as a drug-resistant reservoir [80].

We have observed that a small sub-population (0.1 to 5%) of certain *A. fumigatus* isolates can survive for extended periods and even grow at slow rates in the presence of supra-MIC concentrations of the fungicidal drug voriconazole. In bacteria, tolerance and persistence have been

classically explained by a downregulation of metabolism and cell cycle, which trigger a status of dormancy that permit survival despite the action of the drug. However, recent research in pathogenic bacteria has demonstrated that active metabolic responses are required for persistence [81, 82], and slow-growing persisters have also been detected *in vitro* [83] and *in vivo* [84]. Active metabolism may even be advantageous, as in the case of *Salmonella*, where persisters have been shown to undermine host defences [85]. Interestingly, *C. albicans* AmB persistence has been described to involve downregulation of primary metabolism, but also an increase of stress responses and oxidative defensive mechanisms [86]. We have observed that active growth is possible at two or even three-fold the MIC, and that this growth entails a distinct transcriptional profile. Therefore, this phenomenon is not merely survival of dormant conidia in the presence of the drug, but seems to be an active mechanism that enables a sub-population of certain isolates to withstand the action of voriconazole for an extended period. Indeed, using resazurin (an oxidation-reduction indicator used for the measurement of metabolic activity and proliferation of living cells, which use has been optimised for *A. fumigatus* [87]) we could detect a slight metabolic activity at supra-MIC concentrations (Fig. S7C). This might explain why hypoxia is the only environmental condition that reduced persistence, as in low oxygen the metabolic activity is reduced [80] and the energy generating metabolism changes [88].

We have observed a big difference in growth between liquid media (only microscopic growth) and solid media (macroscopic colonies). We hypothesise that this may be because in agar drug microdepletions around the hyphae would diffuse back much slower than in liquid, giving an advantage to the hyphae in solid media. In addition, there may be a different level of contact of conidia with the drug; in liquid the conidia are completely surrounded, whilst on solid media the conidia just lay on the drug and may escape from it by orientating the germling polarity as they grow.

The concept of persistence entails two intriguing aspects. Firstly, it is an isolate-dependent phenomenon, which means that there must be a genetic basis that underlies persistence. We have shown that the persister isolates do not belong to a specific lineage, suggesting that this feature has not appeared as an evolutionary trait in a lineage of isolates. Recently, it has been described that each *A. fumigatus* strain carries a particular set of accessory genes, which associates with different levels of virulence and drug resistance capacities [89]. In the same vein, we speculate that the presence or absence of certain accessory genes may enable certain isolates to persist in the presence of azoles. Future research will evaluate if this hypothesis is true. A second intriguing aspect of persistence is that it is a sub-population phenomenon, meaning that within an isogenic isolate only a few conidia are able to survive and grow in the presence of the drug. In bacteria, stochastic

expression of key genes has often been proposed as an important underlying cause of persistence [64, 65, 90, 91]. This includes stochastic high expression of genes that directly confer resistance [92] and efflux activity [93]. Similarly, in our RNA-seq analysis we have detected a higher level of expression of genes of the sterol biosynthesis pathway, including *cyp51A*, and of the azole exporter Cdr1B in persister cells. Therefore, it is plausible that stochastic high levels of these genes could generate the capacity to survive for an extended period in the presence of supra-MIC concentrations of voriconazole. Additionally, we detected a higher level of expression of GAG biosynthetic genes, and we have observed that externally added GAG can increase the number of persisters in the isolate PD-104. Interestingly, this polysaccharide did not increase the isolate's MIC, indicating that it does not provide a physical barrier that shields the fungus or that it cannot somehow degrade the drug. Future investigations will aim to unravel why GAG potentiates persistence in PD-104, and not in PD-9, which is interesting as it suggests that there might be multiple persistence mechanisms. GAG is a very relevant *A. fumigatus* virulence factor, with multiple described adhesion and immunosuppressive activities [94, 95], and here we propose that it may have one more important role in potentiating persistence to voriconazole.

In bacterial infections, there is significant evidence supporting a role for the phenomena of tolerance and persistence in antibiotic treatment failure [16, 96]. In contrast, the knowledge about these phenomena in fungal infections is still very scarce. Probably, the best-studied phenomenon is heteroresistance in *Cryptococcus neoformans* and *C. gatii* [97-99], which has been found to be a major cause of treatment failure in cryptococcal meningitis [100-104]. As mentioned above, there is already evidence indicating that fluconazole tolerance can cause treatment failure in invasive candidiasis [17, 21], and limited evidence suggest that caspofungin tolerance may cause treatment failure in *Aspergillus* infections [27]. Here, we show that a voriconazole treatment seems to eliminate persister isolates less efficiently than non-persister isolates in a *Galleria* model of infection. Therefore, this is the very first evidence to suggest that persistence may reduce the efficacy of voriconazole treatment in *A. fumigatus* infections, which would support the hypothesis that persistence might cause therapeutic failure. In addition to such a potential direct effect of persistence on treatment failure, resilience and relapse of persistent strains could associate with the development of antifungal resistance (an effect that has already been shown for bacterial infections, see [105] for references), as it is known that prolonged azole treatment can derive in resistance [106, 107]. As it is well established, development of resistance would cause higher rates of treatment failure, therefore implying an even more relevant role for azole persistence in *A. fumigatus* infections. Of course, much more research is required to reach this conclusion, and we exhort the community to consider and investigate this phenomenon to clarify this important matter.

## MATERIAL and METHODS

### *A. fumigatus* strains and culture conditions.

All isolates utilized in the course of this study are listed in Tables S1 and S8. Briefly, information about the common laboratory strains used can be found in [108], the isolates from Paul Dyer collection are described in [109] and the collection of isolates from the area of Manchester are described in [69]. The third collection of isolates was collected at the TAU medical centre (Tel-Aviv, Israel), these strains were characterized for their resistance profile and *cyp51A* genotype.

Isolates were routinely grown on Potato Dextrose Agar (PDA, Oxoid) for 72 hours to obtain fresh spores for each experiment. *Aspergillus* Minimal Medium (AMM) was prepared following a standard recipe [110]. Sabouraud (Oxoid) and yeast extract glucose (YAG, 2%, 0.5% yeast extract, 1.7% agar, 1X trace elements) media were used in specific experiments.

To evaluate persister growth and determine the MIC, isolates were grown on RPMI-1640 (Sigma) with 35 g/L MOPS (Alfa Aesar) and 2% glucose, pH 7.

Galactosaminogalactan (GAG) was obtained from the *A. fumigatus* Δ*ku80* strain, grown 2-day in 1.5L brian fermenter at room temperature. GAG isolation and purification was carried out as previously described [111]. Briefly, the medium supernatant was collected by filtration and was adjusted to pH 3 by addition of 100 µl 12 M HCl per 100 ml supernatant. Two volumes of precooled ethanol (4°C) were added and GAG was precipitated for 3 h at 4°C. The precipitate was collected by centrifugation for 20 min at 5,000 g at 4°C and subsequently washed twice with 1/10 of the culture volume of 200 mM NaCl for 1 h under agitation (100 rpm). GAG was dialyzed against tap water and twice against purified water (24 h each) and finally lyophilized to dryness and stored at ambient temperature.

### Evaluation of persistence and determination of MICs.

To determine persistence using the disc assay, $4\times10^4$ conidia of each isolate was evenly spread on a solidified RPMI plate (1.5% agar) and 10 µl of 0.8 mg/mL voriconazole or 3.2 mg/mL itraconazole (Acros Organics) was added to a Whatman 6 mm antibiotic assay disc which was placed in the middle of the plate. For *in vitro* treatment with adjuvant and combinatorial drugs, the agents were added to the RPMI medium at the final concentration detailed in each section. Plates were incubated for 5 days at 37 °C.

Minimum inhibitory concentrations (MICs) were calculated using the broth microdilution method according to the EUCAST E.Def. 9.3 instructions [112]. $2.5\times10^4$ conidia were used in each well.

### Evaluation of the conidial survival to voriconazole fungicidal action

To calculate the number of conidia that survived after exposure to high concentration of azoles, full contents of the wells containing the highest concentration of each drug (8 µg/mL) in the broth dilution assays were plated after 48-72 hours incubation on PDA and incubated for 24-48 h at 37 °C.

Microscopic analysis was used to investigate the survival of strains upon withdrawal of voriconazole at single cell level. $1.5\times10^4$ conidia of each strain were inoculated in 300 µL of RPMI in the presence of 8 µg/mL voriconazole (European Pharmacopoeia, -EP- Reference Standard, Merck) and incubated for 48 hours at 37 °C with occasional shaking. The strains were then centrifuged for 4000 RPM for 5 minutes, the media discarded and the conidia resuspended in 2 mL filtered PBS. This wash was repeated three times in total before the conidia were resuspended in 600 µL of drug free RPMI. 300 µL of each suspension, approximately $7.5\times10^3$ conidia, was added into wells of a 96 well plate. The wells were then imaged for 72 hours, every 2 hours, on a Nikon Eclipse Ti microscope, using a Nikon CFI Plan Fluor ELWD 20x/0.45na objective, and captured with a Hamamatsu ORCA-FLASH4.0 LT+ camera (Hamamatsu Photonics) and manipulated using NIS-Elements AR 5.11.01 (Nikon). A video was prepared using Fiji [113].

Microscopy to observe growth at supra-MIC conditions was done in a THUNDER Imager Live Cell microscope, with a HC PL FLUOTAR L 20x/0.40 DRY objective. Images were captured using a Leica-DFC9000GTC-VSC13067 camera and the Las X (Leica application suite) v 3.7 software.

To construct the killing curved, the isolates were inoculated in 10 mL of RPMI containing 4 µg/mL voriconazole. Aliquots for each culture were taken at the time of inoculation (100 µL) and every 24 hours (1 mL). The aliquots were spun at 16,000 ×g for 5 minutes, resupended in 1 mL PBS and vortexed. This was repeated twice to wash off the drug. Finally, conidia were resuspended in 1 mL PBS and a fraction plated on PDA plates (50 µL at time 0h, 100 µL at 24h and 1 mL for 48, 72 and 96 h). The experiment was repeated three times.

To calculate the percentage of germinating conidia, the wells of broth dilution assays containing 2X, 3X MIC and the maximum drug concentration (8 µg/mL) were stained (after reading the MIC) with 10 µg/mL of Calcofluor White (Sigma) for 5 minutes. The entire wells were imaged with a THUNDER Imager Live Cell microscope, using a HC PL FLUOTAR L 20x/0.40 DRY objective, filter conditions: EX:375-435 DCC:455 EM:450-490, a Leica-DFC9000GTC-VSC13067 camera and the Las X (Leica application suite) v 3.7 software. Merged images were analysed using FIJI [113]. Briefly, the merged images were converted to 8-bit, a threshold was set for the images so that the conidia and germlings could be detected over the background (20 to 255). The option analyse particle was then executed, setting a minimum size of 0.04 $inches^2$ (which was found to exclude resting conidia). Wells containing the maximum concentration of the drug, where only resting conidia can be found, were

used to set the background level of detection for each isolate (consisting of aggregates of conidia, impurities and carry over conidiophores from the inoculum). The percentage of germinated conidia/short hyphae was calculated as: (number of counted particles per well – number of counted particles in max drug)/25000 (inoculum).

**Nucleic acid isolation**

For DNA extraction, $10^6$ spores of each *A. fumigatus* isolate were grown overnight on liquid *Aspergillus* minimal medium, filtered through Miracloth paper (Merck), snap frozen and ground in constant presence of liquid nitrogen. Subsequently, DNA was extracted using a standard CTAB method.

For RNA extraction, *A. fumigatus* isolates were grown on 0.45 µm pore nylon membranes (GE Healthcare) placed on RPMI plates and incubated 1 day (without drug) or 5 days (with voriconazole in a disc). Mycelia were scratched using a spatula and immediately frozen and grounded in liquid nitrogen. Subsequently, RNA was extracted and purified with the Plant RNeasy Mini Kit (Qiagen) following the manufacturer's instructions for filamentous fungi, and using on-column DNase treatment.

For fungal burden calculations in *Galleria mellonella*, DNA was extracted from decapitated larvae using the DNeasy Blood & Tissue Kit (Qiagen) following the manufacturer's instruction for animal tissue, with overnight incubation at 56 °C.

***Galleria mellonella* infection**

Sixth-stage instar larval *G. mellonella* moths were purchased from R.J.Mous Livebait (Eigen Haard, The Netherlands). Randomly selected groups of 250-350 mg of weight larvae were injected in the last left proleg with 5 µL of a $2\times10^6$ conidia/mL suspension ($10^4$ conidia/larva) of the correspondent *Aspergillus fumigatus* isolate using Hamilton syringe. 2 hours after infection, relevant groups were injected in the last right proleg with 5 µL of a suspension containing 1600 µg/mL (8 µg/larvae) voriconazole. A PBS control group was subjected to the same treatment, but without fungal infection.

To detect the fungal burden, 500-ng portions of DNA extracted from each larva were subjected to qPCR using the SensiMic SybR Green kit (Bioline). Forward (5′-ACTTCCGCAATGGACGTTAC-3′) and reverse (5′-GGATGTTGTTGGGAATCCAC-3') primers were used to amplify the *A. fumigatus* β-tubulin gene (AFUA_7G00250). The primers designed to amplify the Elongation factor 1-Alpha (Ef-1a) were as follows: forward (5′- AACCTCCTTACAGTGAATCC-3′) and reverse (5′- ATGTTATCTCCGTGCCAG-3′). Standard curves were calculated using different concentrations of fungal and larval gDNA pure

template. Negative controls containing no template DNA were subjected to the same procedure to exclude or detect any possible contamination. Three technical replicates were prepared for each sample. qPCRs were performed using a CFX96 Real-Time System (Bio-rad) with the following thermal cycling parameters: 95°C for 10 min and 40 cycles of 95°C for 15 s and 58°C for 15 s and 72°C for 15 s. The fungal burden was calculated by normalizing the number of fungal genome equivalents (i.e., the number of copies of the tubulin gene) to the larval genome equivalents in the sample (i.e., the number of copies of the Ef-1a gene), as we have reported before [114].

**RNA sequencing (RNA-seq)**

Total RNA was submitted to the Genomic Technologies Core Facility (GTCF) at the University of Manchester, UK. Quality and integrity of the RNA samples were assessed using a 4200 TapeStation (Agilent Technologies) and then libraries generated using the Illumina® Stranded mRNA Prep. Ligation kit (Illumina, Inc.) according to the manufacturer's protocol. Briefly, total RNA (typically 0.025-1ug) was used as input material from which polyadenylated mRNA was purified using poly-T, oligo-attached, magnetic beads. Next, the mRNA was fragmented under elevated temperature and then reverse transcribed into first strand cDNA using random hexamer primers and in the presence of Actinomycin D (thus improving strand specificity whilst mitigating spurious DNA-dependent synthesis). Following removal of the template RNA, second strand cDNA was then synthesized to yield blunt-ended, double-stranded cDNA fragments. Strand specificity was maintained by the incorporation of deoxyuridine triphosphate (dUTP) in place of dTTP to quench the second strand during subsequent amplification. Following a single adenine (A) base addition, adapters with a corresponding, complementary thymine (T) overhang were ligated to the cDNA fragments. Pre-index anchors were then ligated to the ends of the double-stranded cDNA fragments to prepare them for dual indexing. A subsequent PCR amplification step was then used to add the index adapter sequences to create the final cDNA library. The adapter indices enabled the multiplexing of the libraries, which were pooled prior to cluster generation using a cBot instrument. The loaded flow-cell was then paired-end sequenced (76 + 76 cycles, plus indices) on an Illumina HiSeq4000 instrument. Finally, the output data was demultiplexed and BCL-to-Fastq conversion performed using Illumina's bcl2fastq software, version 2.20.0.422.

**RNA-seq analysis**

Unmapped paired-reads of 76bp from the Illumina HiSeq4000 sequencer were checked using a quality control pipeline consisting of FastQC v0.11.3 (http://www.bioinformatics.babraham.ac.uk/projects/fastqc/) and FastQ Screen v0.13.0 (https://www.bioinformatics.babraham.ac.uk/projects/fastq_screen/).

The reads were trimmed to remove any adapter or poor quality sequence using Trimmomatic v0.39 [115]; reads were truncated at a sliding 4bp window, starting 5', with a mean quality <Q20, and removed if the final length was less than 35bp. Additional flags included: 'ILLUMINACLIP:./Truseq3-PE-2_Nextera-PE.fa:2:30:10 SLIDINGWINDOW:4:20 MINLEN:35'.

The filtered reads were mapped either to the *Aspergillus fumigatus* A1163 reference sequence (GCA_000150145.1/ASM15014v1) downloaded from the Ensembl Genomes Fungi v44 [116] or PD-104 a *de novo* assembled genome, using STAR v5.3a [117]. For A1163 reference the genome index was created using the GTF gene annotation also from Ensembl Genomes Fungi v44. For the PD-104 reference GTF gene annotation was generated as described below. A suitable flag for the read length (--sjdbOverhang 75) was used. '--quantMode GeneCounts' was used to generate read counts in genes.

Subsequently, PD-104 reads were aligned to the recently generated pan-genome [62] using Salmon v1.6.0 (additional parameters for salmon quant: --gcBias (corrects for any GC biases in samples) -l ISR (inward / stranded / reverse read pairs)).

Normalisation and differential expression analysis was performed using DESeq2 v1.34.0 [118] on R v4.1.2 (R Core Team. 2021. R: A Language and Environment for Statistical Computing. https://www.R-project.org/). Log fold change shrinkage was applied using the lfcShrink function along with the "apeglm" algorithm [119].

**DNA sequencing (Illumina DNA Prep)**

Genomic DNA was submitted to the Genomic Technologies Core Facility (GTCF) at the University of Manchester. Sequencing libraries were generated using on-bead tagmentation chemistry with the llumina® DNA Prep, (M) Tagmentation Kit (Illumina, Inc.) according to the manufacturer's protocol. Briefly, bead-linked transposomes were used to mediate the simultaneous fragmentation of gDNA (100-500ng) and the addition of Illumina sequencing primers. Next, reduced-cycle PCR amplification was used to amplify sequencing ready DNA fragments and to add the indices and adapters. Finally, sequencing-ready fragments were washed and pooled prior to paired-end sequencing (151 + 151 cycles, plus indices) on an Illumina NextSeq500 instrument. Finally, the output data were demultiplexed (allowing one mismatch) and BCL-to-Fastq conversion performed using Illumina's bcl2fastq software, version 2.20.0.422.

The RNA data is stored in Array Express, accession E-MTAB-11547 (https://www.ebi.ac.uk/arrayexpress/experiments/E-MTAB-11547).

**Method for de novo genome assembly of genomes.**

The method mentions PD-104 as an example, but is relevant to the remaining isolates.

Unmapped paired-end reads of 149bp from an Illumina NextSeq500 sequencer were checked using a quality control pipeline consisting of FastQC v0.11.3 (http://www.bioinformatics.babraham.ac.uk/projects/fastqc/) and FastQ Screen v0.13.0 (https://www.bioinformatics.babraham.ac.uk/projects/fastq_screen/).

The reads were trimmed to remove any adapter or poor quality sequence using Trimmomatic v0.39 [115]. Within the first or last 30bp of a read bases were removed if quality was <30. A sliding 2bp window, starting 5', scanned the reads and truncated at a window with a mean quality <Q20. Reads were removed if the final length was less than 100bp. Additional flags included: 'ILLUMINACLIP:../Truseq3_Nextera-PE.fa:2:30:10 LEADING:30 TRAILING:30 SLIDINGWINDOW:2:20 MINLEN:100'.

Genome assembly was performed using Megahit v1.2.9 [120], using the flag '--no-mercy'. This resulted in 799 contigs, total 28659847 bp, min 202 bp, max 401152 bp, avg 35869 bp, N50 97740 bp. In comparison A1163 has 55 contigs total 29205420 bp.

Quast v5.0.2 [121] was used to determine the quality of the assembly. An example of the PD-104 results can be found in Table S9.

ProtHint v2.5.0 and GeneMark-EP+ v4.68_lic [122] were used for gene annotation. ProtHint was used to generate the evidence for coding genes in combination with fungal protein download from OrthoDb v10. ProtHint generates two main outputs: `prothint.gff` a GFF file with all reported hints (introns, starts and stops), and `evidence.gff` high confidence subset of `prothint.gff` which is suitable for the GeneMark-EP Plus mode. GeneMark-EP+ was used to generate a GTF file of candidate genes for the PD-104 assembly. Additional parameters were set '--max_intron 200 --max_intergenic 100000 --min_contig=1000 --fungus'.

In order to determine the function of the novel genes, initially a reciprocal best hit strategy was used comparing protein sequence from PD-104 (using the GeneMark Perl script 'get_sequence_from_GTF.pl' with the GTF file and assembled contigs) and A1163 (proteins downloaded from Ensembl Genomes Fungi release 51: http://ftp.ensemblgenomes.org/pub/fungi/release-51/fasta/aspergillus_fumigatusa1163/pep/Aspergillus_fumigatusa1163.ASM15014v1.pep.all.fa.gz).

The best match method was run using proteinortho v6.0.31 [123], which by default uses the program Diamond v2.0.13 [124] to identify protein matches ('-p=diamond'). The flag '-sim=1' was set to obtain best reciprocal matches only.

**Construction of Phylogenetic tree:**

Pre-alignment, the reference Af293 genome [125] was masked to remove low-complexity regions using RepeatMasker (http://www.repeatmasker.org/) v.4.1.2-p1 and the Dfam repeat database

[126] release 3.5. Quality-checked DNA sequencing reads from the recently generated pan-genome study [62] were combined with the reads generated from this study and underwent alignment to the masked reference Af293 genome, using BWA-MEM [127] v.0.7.17-r1188. Alignment files were then converted to the sorted BAM format using SAMtools [128] v.1.10. Variant calling was then performed with GATK HaplotypeCaller [129] v.4.0. All variant calls with a genotype quality less than 50 were removed and low-confidence SNPs were converted to missing data if they met one of the follow criteria: DP<10|| RMSMappingQuality<40.0|| QualByDepth<2.0|| FisherStrand>60.0|| ABHom<0.9. Each newly generated VCF file was then compressed, indexed and then merged into a single file using VCFtools [130] v.0.1.16. This data was then converted into a relaxed interleaved Phylip format using vcf2phylip [131] v2.8 and RAxML [132] v.8.2.12, under rapid bootstrap analysis using 1,000 replicates with the GTRCAT model, was employed to generate maximum-likelihood phylogenies to test whether persistence is lineage-specific. Phylogenetic trees with overlaying metadata were generated using iTOL [133] v.6.5.4.

**ACKNOWLEGDGEMENTS**

We are deeply grateful to Prof Paul Dyer, who kindly gifted to us the collection of isolates that have been used in this study. We would like to thank Diego Megías and Clara Martín at ISCIII for their help with the microscopy. We acknowledge the use of the Genomic Technologies Facility (Faculty of Biology Medicine and Health, University of Manchester) for the DNA and RNA sequencing. Help and support from members of MFIG and LRIM is greatly appreciated.

JA is funded by an Atracción de Talento Modalidad 1 (020-T1/BMD-200) contract of the Madrid Regional Government (CAM). JS has been funded by a BSAC Scholarship (bsac-2016-0049). CV was funded by FAPESP (2108/00715-3 and 2020/01131-5). GHG has been funded by FAPESP (2016/07870-9 and 2021/04977-5) and CNPq (301058/2019-9 and 404735/2018-5). SG was co-funded by the NIHR Manchester Research Centre and the Fungal Infection Trust.

**DATA AVAILABILITY**

Transcriptomic data is available in Array Express (https://www.ebi.ac.uk/arrayexpress/experiments/E-MTAB-11547). All raw data is available upon reasonable request.

**REFERENCES**

1. Latgé, J.-P. and G. Chamilos, *Aspergillus fumigatus and Aspergillosis in 2019*. Clinical Microbiology Reviews, 2019. **33**(1) DOI: 10.1128/cmr.00140-18.

2. Perfect, J.R., *The antifungal pipeline: a reality check.* Nat Rev Drug Discov, 2017. **16**(9): p. 603-616 DOI: 10.1038/nrd.2017.46.
3. Ruping, M.J., J.J. Vehreschild, and O.A. Cornely, *Antifungal treatment strategies in high risk patients.* Mycoses, 2008. **51 Suppl 2**: p. 46-51 DOI: 10.1111/j.1439-0507.2008.01572.x.
4. Koehler, P., et al., *Defining and managing COVID-19-associated pulmonary aspergillosis: the 2020 ECMM/ISHAM consensus criteria for research and clinical guidance.* The Lancet Infectious Diseases, 2021. **21**(6): p. e149-e162 DOI: 10.1016/s1473-3099(20)30847-1.
5. Marr, K.A., et al., *Aspergillosis Complicating Severe Coronavirus Disease.* Emerging Infectious Diseases, 2021. **27**(1): p. 18-25 DOI: 10.3201/eid2701.202896.
6. Helleberg, M., M. Steensen, and M.C. Arendrup, *Invasive aspergillosis in patients with severe COVID-19 pneumonia.* Clinical Microbiology and Infection, 2021. **27**(1): p. 147-148 DOI: 10.1016/j.cmi.2020.07.047.
7. Lowes, D., et al., *Predictors of mortality in chronic pulmonary aspergillosis.* Eur Respir J, 2017. **49**(2) DOI: 10.1183/13993003.01062-2016.
8. Brown, G.D., et al., *Hidden killers: human fungal infections.* Sci Transl Med, 2012. **4**(165): p. 165rv13 DOI: 10.1126/scitranslmed.3004404.
9. Ballou, L., *Fungal diseases deserve our attention.* Nature Microbiology Community, 2017. http://go.nature.com/2jlKFYZ.
10. Fisher, M.C., et al., *Worldwide emergence of resistance to antifungal drugs challenges human health and food security.* Science, 2018. **360**(6390): p. 739-742 DOI: 10.1126/science.aap7999.
11. Verweij, P.E., et al., *International expert opinion on the management of infection caused by azole-resistant Aspergillus fumigatus.* Drug Resist Updat, 2015. **21-22**: p. 30-40 DOI: 10.1016/j.drup.2015.08.001.
12. Lestrade, P.P., et al., *Voriconazole Resistance and Mortality in Invasive Aspergillosis: A Multicenter Retrospective Cohort Study.* Clin Infect Dis, 2019. **68**(9): p. 1463-1471 DOI: 10.1093/cid/ciy859.
13. Meis, J.F., et al., *Clinical implications of globally emerging azole resistance in Aspergillus fumigatus.* Philos Trans R Soc Lond B Biol Sci, 2016. **371**(1709) DOI: 10.1098/rstb.2015.0460.
14. Galiger, C., et al., *Assessment of efficacy of antifungals against Aspergillus fumigatus: value of real-time bioluminescence imaging.* Antimicrob Agents Chemother, 2013. **57**(7): p. 3046-59 DOI: 10.1128/AAC.01660-12.
15. Heo, S.T., et al., *Changes in In Vitro Susceptibility Patterns of Aspergillus to Triazoles and Correlation With Aspergillosis Outcome in a Tertiary Care Cancer Center, 1999–2015.* Clinical Infectious Diseases, 2017. **65**(2): p. 216-225 DOI: 10.1093/cid/cix297.
16. Leong, J.M., et al., *Antibiotic tolerance.* PLOS Pathogens, 2020. **16**(10) DOI: 10.1371/journal.ppat.1008892.
17. Levinson, T., et al., *Impact of tolerance to fluconazole on treatment response in Candida albicans bloodstream infection.* Mycoses, 2020. **64**(1): p. 78-85 DOI: 10.1111/myc.13191.
18. Brauner, A., et al., *Distinguishing between resistance, tolerance and persistence to antibiotic treatment.* Nature Reviews Microbiology, 2016. **14**(5): p. 320-330 DOI: 10.1038/nrmicro.2016.34.
19. Balaban, N.Q., et al., *Definitions and guidelines for research on antibiotic persistence.* Nature Reviews Microbiology, 2019. **17**(7): p. 441-448 DOI: 10.1038/s41579-019-0196-3.
20. Meylan, S., I.W. Andrews, and J.J. Collins, *Targeting Antibiotic Tolerance, Pathogen by Pathogen.* Cell, 2018. **172**(6): p. 1228-1238 DOI: 10.1016/j.cell.2018.01.037.
21. Rosenberg, A., et al., *Antifungal tolerance is a subpopulation effect distinct from resistance and is associated with persistent candidemia.* Nature Communications, 2018. **9**(1) DOI: 10.1038/s41467-018-04926-x.

22. Martos, A.I., et al., *Evaluation of the Etest method for susceptibility testing of Aspergillus spp. and Fusarium spp. to three echinocandins.* Med Mycol, 2010. **48**(6): p. 858-61 DOI: 10.3109/13693781003586943.
23. Lass-Florl, C., et al., *Antifungal susceptibility testing in Aspergillus spp. according to EUCAST methodology.* Med Mycol, 2006. **44**(Supplement_1): p. S319-S325 DOI: 10.1080/13693780600779401.
24. Bleichrodt, R.J., et al., *Cell Wall Composition Heterogeneity between Single Cells in Aspergillus fumigatus Leads to Heterogeneous Behavior during Antifungal Treatment and Phagocytosis.* mBio, 2020. **11**(3) DOI: 10.1128/mBio.03015-19.
25. Wagener, J. and V. Loiko, *Recent Insights into the Paradoxical Effect of Echinocandins.* Journal of Fungi, 2017. **4**(1) DOI: 10.3390/jof4010005.
26. Valero, C., et al., *The Caspofungin Paradoxical Effect is a Tolerant "Eagle Effect" in the Filamentous Fungal Pathogen Aspergillus fumigatus.* mBio, 2022 DOI: 10.1128/mbio.00447-22.
27. Aruanno, M., E. Glampedakis, and F. Lamoth, *Echinocandins for the Treatment of Invasive Aspergillosis: from Laboratory to Bedside.* Antimicrobial Agents and Chemotherapy, 2019. **63**(8) DOI: 10.1128/aac.00399-19.
28. Gheith, S., et al., *In vitro susceptibility to amphotericin B, itraconazole, voriconazole, posaconazole and caspofungin of Aspergillus spp. isolated from patients with haematological malignancies in Tunisia.* Springerplus, 2014. **3**: p. 19 DOI: 10.1186/2193-1801-3-19.
29. Geißel, B., et al., *Azole-induced cell wall carbohydrate patches kill Aspergillus fumigatus.* Nature Communications, 2018. **9**(1) DOI: 10.1038/s41467-018-05497-7.
30. Majoros, L. and G. Kardos, *Fungicidal Activity of Azole Antifungal Agents.* Anti-Infective Agents in Medicinal Chemistry, 2008. **7**(2): p. 118-125 DOI: 10.2174/187152108783954623.
31. Manavathu, E.K., J.L. Cutright, and P.H. Chandrasekar, *Organism-Dependent Fungicidal Activities of Azoles.* Antimicrobial Agents and Chemotherapy, 1998. **42**(11): p. 3018-3021 DOI: 10.1128/aac.42.11.3018.
32. Wang, F., et al., *Transcription in fungal conidia before dormancy produces phenotypically variable conidia that maximize survival in different environments.* Nature Microbiology, 2021. **6**(8): p. 1066-1081 DOI: 10.1038/s41564-021-00922-y.
33. Gefen, O., et al., *TDtest: easy detection of bacterial tolerance and persistence in clinical isolates by a modified disk-diffusion assay.* Sci Rep, 2017. **7**: p. 41284 DOI: 10.1038/srep41284.
34. Gonzalez-Jimenez, I., et al., *Are Point Mutations in HMG-CoA Reductases (Hmg1 and Hmg2) a Step towards Azole Resistance in Aspergillus fumigatus?* Molecules, 2021. **26**(19) DOI: 10.3390/molecules26195975.
35. Zhang, J., et al., *Evolution of cross-resistance to medical triazoles in Aspergillus fumigatus through selection pressure of environmental fungicides.* Proceedings of the Royal Society B: Biological Sciences, 2017. **284**(1863) DOI: 10.1098/rspb.2017.0635.
36. Windels, E.M., et al., *Bacterial persistence promotes the evolution of antibiotic resistance by increasing survival and mutation rates.* The ISME Journal, 2019. **13**(5): p. 1239-1251 DOI: 10.1038/s41396-019-0344-9.
37. Sebastian, J., et al., *De Novo Emergence of Genetically Resistant Mutants of Mycobacterium tuberculosis from the Persistence Phase Cells Formed against Antituberculosis Drugs In Vitro.* Antimicrobial Agents and Chemotherapy, 2017. **61**(2) DOI: 10.1128/aac.01343-16.
38. Suh, M.-J., et al., *Development stage-specific proteomic profiling uncovers small, lineage specific proteins most abundant in the Aspergillus fumigatus conidial proteome.* Proteome Science, 2012. **10**(1) DOI: 10.1186/1477-5956-10-30.
39. Mowat, E., et al., *Phase-dependent antifungal activity against Aspergillus fumigatus developing multicellular filamentous biofilms.* Journal of Antimicrobial Chemotherapy, 2008. **62**(6): p. 1281-1284 DOI: 10.1093/jac/dkn402.

40. Yu, J.S.L., et al., *Microbial communities form rich extracellular metabolomes that foster metabolic interactions and promote drug tolerance.* Nature Microbiology, 2022. **7**(4): p. 542-555 DOI: 10.1038/s41564-022-01072-5.
41. Day, A.M. and J. Quinn, *Stress-Activated Protein Kinases in Human Fungal Pathogens.* Frontiers in Cellular and Infection Microbiology, 2019. **9** DOI: 10.3389/fcimb.2019.00261.
42. Hagiwara, D., et al., *Signaling pathways for stress responses and adaptation in Aspergillus species: stress biology in the post-genomic era.* Bioscience, Biotechnology, and Biochemistry, 2016. **80**(9): p. 1667-1680 DOI: 10.1080/09168451.2016.1162085.
43. Manfiolli, A.O., et al., *Aspergillus fumigatus High Osmolarity Glycerol Mitogen Activated Protein Kinases SakA and MpkC Physically Interact During Osmotic and Cell Wall Stresses.* Frontiers in Microbiology, 2019. **10** DOI: 10.3389/fmicb.2019.00918.
44. Takahashi, H., et al., *Global gene expression reveals stress-responsive genes in Aspergillus fumigatus mycelia.* BMC Genomics, 2017. **18**(1) DOI: 10.1186/s12864-017-4316-z.
45. Berman, J. and D.J. Krysan, *Drug resistance and tolerance in fungi.* Nat Rev Microbiol, 2020 DOI: 10.1038/s41579-019-0322-2.
46. Cowen, L.E., et al., *Harnessing Hsp90 function as a powerful, broadly effective therapeutic strategy for fungal infectious disease.* Proceedings of the National Academy of Sciences, 2009. **106**(8): p. 2818-2823 DOI: 10.1073/pnas.0813394106.
47. Lamoth, F., et al., *Antifungal activity of compounds targeting the Hsp90-calcineurin pathway against various mould species.* Journal of Antimicrobial Chemotherapy, 2015. **70**(5): p. 1408-1411 DOI: 10.1093/jac/dku549.
48. Juvvadi, P.R., F. Lamoth, and W.J. Steinbach, *Calcineurin as a multifunctional regulator: Unraveling novel functions in fungal stress responses, hyphal growth, drug resistance, and pathogenesis.* Fungal Biology Reviews, 2014. **28**(2-3): p. 56-69 DOI: 10.1016/j.fbr.2014.02.004.
49. Sestari, S.J., et al., *Inhibition of protein kinase A affects Paracoccidioides lutzii dimorphism.* International Journal of Biological Macromolecules, 2018. **113**: p. 1214-1220 DOI: 10.1016/j.ijbiomac.2018.03.023.
50. Chen, S.C.A., R.E. Lewis, and D.P. Kontoyiannis, *Direct effects of non-antifungal agents used in cancer chemotherapy and organ transplantation on the development and virulence of Candida and Aspergillus species.* Virulence, 2014. **2**(4): p. 280-295 DOI: 10.4161/viru.2.4.16764.
51. Weichert, M., et al., *Functional Coupling between the Unfolded Protein Response and Endoplasmic Reticulum/Golgi Ca2+-ATPases Promotes Stress Tolerance, Cell Wall Biosynthesis, and Virulence of Aspergillus fumigatus.* mBio, 2020. **11**(3) DOI: 10.1128/mBio.01060-20.
52. Istvan, E.S., *Structural Mechanism for Statin Inhibition of HMG-CoA Reductase.* Science, 2001. **292**(5519): p. 1160-1164 DOI: 10.1126/science.1059344.
53. Qiao, J., et al., *Antifungal activity of statins against Aspergillus species.* Med Mycol, 2007. **45**(7): p. 589-93 DOI: 10.1080/13693780701397673.
54. Silva, L.V., et al., *Milbemycins: More than Efflux Inhibitors for Fungal Pathogens.* Antimicrobial Agents and Chemotherapy, 2012. **57**(2): p. 873-886 DOI: 10.1128/aac.02040-12.
55. Esquivel, B.D., et al., *Characterization of the Efflux Capability and Substrate Specificity of Aspergillus fumigatus PDR5-like ABC Transporters Expressed in Saccharomyces cerevisiae.* mBio, 2020. **11**(2) DOI: 10.1128/mBio.00338-20.
56. Gonzalez-Jimenez, I., et al., *A Cyp51B Mutation Contributes to Azole Resistance in Aspergillus fumigatus.* Journal of Fungi, 2020. **6**(4) DOI: 10.3390/jof6040315.
57. Rybak, J.M., et al., *Mutations in hmg1, Challenging the Paradigm of Clinical Triazole Resistance in Aspergillus fumigatus.* mBio, 2019. **10**(2) DOI: 10.1128/mBio.00437-19.

58. Furukawa, T., et al., *The negative cofactor 2 complex is a key regulator of drug resistance in Aspergillus fumigatus.* Nat Commun, 2020. **11**(1): p. 427 DOI: 10.1038/s41467-019-14191-1.
59. Hulsen, T., J. de Vlieg, and W. Alkema, *BioVenn - a web application for the comparison and visualization of biological lists using area-proportional Venn diagrams.* BMC Genomics, 2008. **9**: p. 488 DOI: 10.1186/1471-2164-9-488.
60. Amos, B., et al., *VEuPathDB: the eukaryotic pathogen, vector and host bioinformatics resource center.* Nucleic Acids Research, 2022. **50**(D1): p. D898-D911 DOI: 10.1093/nar/gkab929.
61. Peyrusson, F., et al., *Intracellular Staphylococcus aureus persisters upon antibiotic exposure.* Nature Communications, 2020. **11**(1) DOI: 10.1038/s41467-020-15966-7.
62. Rhodes, J., et al., *Population genomics confirms acquisition of drug-resistant Aspergillus fumigatus infection by humans from the environment.* Nature Microbiology, 2022 DOI: 10.1038/s41564-022-01091-2.
63. Szklarczyk, D., et al., *The STRING database in 2021: customizable protein-protein networks, and functional characterization of user-uploaded gene/measurement sets.* Nucleic Acids Res, 2021. **49**(D1): p. D605-D612 DOI: 10.1093/nar/gkaa1074.
64. Rossi, N.A., I. El Meouche, and M.J. Dunlop, *Forecasting cell fate during antibiotic exposure using stochastic gene expression.* Communications Biology, 2019. **2**(1) DOI: 10.1038/s42003-019-0509-0.
65. Urbaniec, J., et al., *Phenotypic heterogeneity in persisters: a novel 'hunker' theory of persistence.* FEMS Microbiology Reviews, 2022. **46**(1) DOI: 10.1093/femsre/fuab042.
66. Fraczek, M.G., et al., *The cdr1B efflux transporter is associated with non-cyp51a-mediated itraconazole resistance in Aspergillus fumigatus* Journal of Antimicrobial Chemotherapy, 2013. **68**(7): p. 1486-1496 DOI: 10.1093/jac/dkt075.
67. Bamford, N.C., et al., *Sph3 Is a Glycoside Hydrolase Required for the Biosynthesis of Galactosaminogalactan in Aspergillus fumigatus.* Journal of Biological Chemistry, 2015. **290**(46): p. 27438-27450 DOI: 10.1074/jbc.M115.679050.
68. Lee, M.J., et al., *Deacetylation of Fungal Exopolysaccharide Mediates Adhesion and Biofilm Formation.* mBio, 2016. **7**(2) DOI: 10.1128/mBio.00252-16.
69. Bromley, M.J., et al., *Occurrence of azole-resistant species of Aspergillus in the UK environment.* J Glob Antimicrob Resist, 2014. **2**(4): p. 276-279 DOI: 10.1016/j.jgar.2014.05.004.
70. Gonzalez-Jimenez, I., et al., *Multiresistance to Nonazole Fungicides in Aspergillus fumigatus TR34/L98H Azole-Resistant Isolates.* Antimicrobial Agents and Chemotherapy, 2021. **65**(9) DOI: 10.1128/aac.00642-21.
71. Forastiero, A., et al., *In vivo efficacy of voriconazole and posaconazole therapy in a novel invertebrate model of Aspergillus fumigatus infection.* International Journal of Antimicrobial Agents, 2015. **46**(5): p. 511-517 DOI: 10.1016/j.ijantimicag.2015.07.007.
72. Gomez-Lopez, A., et al., *An invertebrate model to evaluate virulence in Aspergillus fumigatus: The role of azole resistance.* Medical Mycology, 2014. **52**(3): p. 311-319 DOI: 10.1093/mmy/myt022.
73. Jemel, S., et al., *In Vivo Efficacy of Voriconazole in a Galleria mellonella Model of Invasive Infection Due to Azole-Susceptible or Resistant Aspergillus fumigatus Isolates.* Journal of Fungi, 2021. **7**(12) DOI: 10.3390/jof7121012.
74. Hobby, G.L., K. Meyer, and E. Chaffee, *Observations on the Mechanism of Action of Penicillin.* Experimental Biology and Medicine, 1942. **50**(2): p. 281-285 DOI: 10.3181/00379727-50-13773.
75. Bigger, J., *Treatment of Staphylococcal Infections with Penicillin by Intermittent Sterilisation.* The Lancet, 1944. **244**(6320): p. 497-500 DOI: 10.1016/s0140-6736(00)74210-3.

76. Cohen, Nadia R., Michael A. Lobritz, and James J. Collins, *Microbial Persistence and the Road to Drug Resistance.* Cell Host & Microbe, 2013. **13**(6): p. 632-642 DOI: 10.1016/j.chom.2013.05.009.
77. Huemer, M., et al., *Antibiotic resistance and persistence—Implications for human health and treatment perspectives.* EMBO reports, 2020. **21**(12) DOI: 10.15252/embr.202051034.
78. LaFleur, M.D., C.A. Kumamoto, and K. Lewis, *Candida albicans Biofilms Produce Antifungal-Tolerant Persister Cells.* Antimicrobial Agents and Chemotherapy, 2006. **50**(11): p. 3839-3846 DOI: 10.1128/aac.00684-06.
79. Hobman, T.C., et al., *Fungal persister cells: The basis for recalcitrant infections?* PLOS Pathogens, 2018. **14**(10) DOI: 10.1371/journal.ppat.1007301.
80. Kowalski, C.H., et al., *Fungal biofilm architecture produces hypoxic microenvironments that drive antifungal resistance.* Proceedings of the National Academy of Sciences, 2020. **117**(36): p. 22473-22483 DOI: 10.1073/pnas.2003700117.
81. Wilmaerts, D., et al., *General Mechanisms Leading to Persister Formation and Awakening.* Trends in Genetics, 2019. **35**(6): p. 401-411 DOI: 10.1016/j.tig.2019.03.007.
82. Orman, M.A. and M.P. Brynildsen, *Dormancy Is Not Necessary or Sufficient for Bacterial Persistence.* Antimicrobial Agents and Chemotherapy, 2013. **57**(7): p. 3230-3239 DOI: 10.1128/aac.00243-13.
83. Wakamoto, Y., et al., *Dynamic Persistence of Antibiotic-Stressed Mycobacteria.* Science, 2013. **339**(6115): p. 91-95 DOI: 10.1126/science.1229858.
84. Claudi, B., et al., *Phenotypic Variation of Salmonella in Host Tissues Delays Eradication by Antimicrobial Chemotherapy.* Cell, 2014. **158**(4): p. 722-733 DOI: 10.1016/j.cell.2014.06.045.
85. Stapels, D.A.C., et al., *Salmonella persisters undermine host immune defenses during antibiotic treatment.* Science, 2018. **362**(6419): p. 1156-1160 DOI: 10.1126/science.aat7148.
86. Li, P., et al., *Delicate Metabolic Control and Coordinated Stress Response Critically Determine Antifungal Tolerance of Candida albicans Biofilm Persisters.* Antimicrobial Agents and Chemotherapy, 2015. **59**(10): p. 6101-6112 DOI: 10.1128/aac.00543-15.
87. Monteiro, M.C., et al., *A New Approach to Drug Discovery: High-Throughput Screening of Microbial Natural Extracts against Aspergillus fumigatus Using Resazurin* Journal of Biomolecular Screening, 2012. **17**(4): p. 542-549 DOI: 10.1177/1087057111433459.
88. Hillmann, F., E. Shekhova, and O. Kniemeyer, *Insights into the cellular responses to hypoxia in filamentous fungi.* Current Genetics, 2015. **61**(3): p. 441-455 DOI: 10.1007/s00294-015-0487-9.
89. Barber, A.E., et al., *Aspergillus fumigatus pan-genome analysis identifies genetic variants associated with human infection.* Nature Microbiology, 2021. **6**(12): p. 1526-1536 DOI: 10.1038/s41564-021-00993-x.
90. Manuse, S., et al., *Bacterial persisters are a stochastically formed subpopulation of low-energy cells.* PLOS Biology, 2021. **19**(4) DOI: 10.1371/journal.pbio.3001194.
91. Zalis, E.A., et al., *Stochastic Variation in Expression of the Tricarboxylic Acid Cycle Produces Persister Cells.* mBio, 2019. **10**(5) DOI: 10.1128/mBio.01930-19.
92. El Meouche, I., Y. Siu, and M.J. Dunlop, *Stochastic expression of a multiple antibiotic resistance activator confers transient resistance in single cells.* Scientific Reports, 2016. **6**(1) DOI: 10.1038/srep19538.
93. Pu, Y., et al., *Enhanced Efflux Activity Facilitates Drug Tolerance in Dormant Bacterial Cells.* Molecular Cell, 2016. **62**(2): p. 284-294 DOI: 10.1016/j.molcel.2016.03.035.
94. Fontaine, T., et al., *Galactosaminogalactan, a New Immunosuppressive Polysaccharide of Aspergillus fumigatus.* PLoS Pathogens, 2011. **7**(11) DOI: 10.1371/journal.ppat.1002372.
95. Speth, C., et al., *Galactosaminogalactan (GAG) and its multiple roles in Aspergillus pathogenesis.* Virulence, 2019. **10**(1): p. 976-983 DOI: 10.1080/21505594.2019.1568174.
96. Fisher, R.A., B. Gollan, and S. Helaine, *Persistent bacterial infections and persister cells.* Nature Reviews Microbiology, 2017. **15**(8): p. 453-464 DOI: 10.1038/nrmicro.2017.42.

97. Mondon, P., et al., *Heteroresistance to fluconazole and voriconazole in Cryptococcus neoformans.* Antimicrob Agents Chemother, 1999. **43**(8): p. 1856-61 DOI: 10.1128/AAC.43.8.1856.
98. Yamazumi, T., et al., *Characterization of Heteroresistance to Fluconazole among Clinical Isolates of Cryptococcus neoformans.* Journal of Clinical Microbiology, 2003. **41**(1): p. 267-272 DOI: 10.1128/jcm.41.1.267-272.2003.
99. Varma, A. and K.J. Kwon-Chung, *Heteroresistance of Cryptococcus gattii to Fluconazole.* Antimicrobial Agents and Chemotherapy, 2010. **54**(6): p. 2303-2311 DOI: 10.1128/aac.00153-10.
100. Stone, N.R.H., et al., *Dynamic ploidy changes drive fluconazole resistance in human cryptococcal meningitis.* Journal of Clinical Investigation, 2019. **129**(3): p. 999-1014 DOI: 10.1172/jci124516.
101. Barsh, G.S., et al., *A non-canonical RNA degradation pathway suppresses RNAi-dependent epimutations in the human fungal pathogen Mucor circinelloides.* PLOS Genetics, 2017. **13**(3) DOI: 10.1371/journal.pgen.1006686.
102. Ferreira, G.F. and D.A. Santos, *Heteroresistance and fungi.* Mycoses, 2017. **60**(9): p. 562-568 DOI: 10.1111/myc.12639.
103. Sionov, E., et al., *Heteroresistance to Fluconazole in Cryptococcus neoformans Is Intrinsic and Associated with Virulence.* Antimicrobial Agents and Chemotherapy, 2009. **53**(7): p. 2804-2815 DOI: 10.1128/aac.00295-09.
104. Todd, R.T. and A. Selmecki, *Expandable and reversible copy number amplification drives rapid adaptation to antifungal drugs.* eLife, 2020. **9** DOI: 10.7554/eLife.58349.
105. Windels, E.M., et al., *Antibiotics: Combatting Tolerance To Stop Resistance.* mBio, 2019. **10**(5) DOI: 10.1128/mBio.02095-19.
106. Tashiro, M., et al., *Correlation between Triazole Treatment History and Susceptibility in Clinically Isolated Aspergillus fumigatus.* Antimicrobial Agents and Chemotherapy, 2012. **56**(9): p. 4870-4875 DOI: 10.1128/Aac.00514-12.
107. Kamei, K., et al., *High detection rate of azole-resistant Aspergillus fumigatus after treatment with azole antifungal drugs among patients with chronic pulmonary aspergillosis in a single hospital setting with low azole resistance.* Medical Mycology, 2020 DOI: 10.1093/mmy/myaa052.
108. Bertuzzi, M., et al., *On the lineage of Aspergillus fumigatus isolates in common laboratory use.* Medical Mycology, 2021. **59**(1): p. 7-13 DOI: 10.1093/mmy/myaa075.
109. Swilaiman, S.S., et al., *Global Sexual Fertility in the Opportunistic Pathogen Aspergillus fumigatus and Identification of New Supermater Strains.* J Fungi (Basel), 2020. **6**(4) DOI: 10.3390/jof6040258.
110. Moreno, M.A., et al., *Culture conditions for zinc- and pH-regulated gene expression studies in Aspergillus fumigatus.* Int Microbiol, 2007. **10**(3): p. 187-92.
111. Gressler, M., et al., *Definition of the Anti-inflammatory Oligosaccharides Derived From the Galactosaminogalactan (GAG) From Aspergillus fumigatus.* Frontiers in Cellular and Infection Microbiology, 2019. **9** DOI: 10.3389/fcimb.2019.00365.
112. Arendrup, M.C., et al., *EUCAST technical note on isavuconazole breakpoints for Aspergillus, itraconazole breakpoints for Candida and updates for the antifungal susceptibility testing method documents.* Clinical Microbiology and Infection, 2016. **22**(6): p. 571.e1-571.e4 DOI: 10.1016/j.cmi.2016.01.017.
113. Schindelin, J., et al., *Fiji: an open-source platform for biological-image analysis.* Nature Methods, 2012. **9**(7): p. 676-682 DOI: 10.1038/nmeth.2019.
114. Scott, J., et al., *Pseudomonas aeruginosa-Derived Volatile Sulfur Compounds Promote Distal Aspergillus fumigatus Growth and a Synergistic Pathogen-Pathogen Interaction That Increases Pathogenicity in Co-infection.* Front Microbiol, 2019. **10**: p. 2311 DOI: 10.3389/fmicb.2019.02311.

115. Bolger, A.M., M. Lohse, and B. Usadel, *Trimmomatic: a flexible trimmer for Illumina sequence data.* Bioinformatics, 2014. **30**(15): p. 2114-2120 DOI: 10.1093/bioinformatics/btu170.
116. Howe, K.L., et al., *Ensembl Genomes 2020—enabling non-vertebrate genomic research.* Nucleic Acids Research, 2020. **48**(D1): p. D689-D695 DOI: 10.1093/nar/gkz890.
117. Dobin, A., et al., *STAR: ultrafast universal RNA-seq aligner.* Bioinformatics, 2013. **29**(1): p. 15-21 DOI: 10.1093/bioinformatics/bts635.
118. Love, M.I., W. Huber, and S. Anders, *Moderated estimation of fold change and dispersion for RNA-seq data with DESeq2.* Genome Biology, 2014. **15**(12) DOI: 10.1186/s13059-014-0550-8.
119. Zhu, A., et al., *Heavy-tailed prior distributions for sequence count data: removing the noise and preserving large differences.* Bioinformatics, 2019. **35**(12): p. 2084-2092 DOI: 10.1093/bioinformatics/bty895.
120. Li, D., et al., *MEGAHIT: an ultra-fast single-node solution for large and complex metagenomics assembly via succinct de Bruijn graph.* Bioinformatics, 2015. **31**(10): p. 1674-1676 DOI: 10.1093/bioinformatics/btv033.
121. Gurevich, A., et al., *QUAST: quality assessment tool for genome assemblies.* Bioinformatics, 2013. **29**(8): p. 1072-1075 DOI: 10.1093/bioinformatics/btt086.
122. Brůna, T., A. Lomsadze, and M. Borodovsky, *GeneMark-EP+: eukaryotic gene prediction with self-training in the space of genes and proteins.* NAR Genomics and Bioinformatics, 2020. **2**(2) DOI: 10.1093/nargab/lqaa026.
123. Lechner, M., et al., *Proteinortho: Detection of (Co-)orthologs in large-scale analysis.* BMC Bioinformatics, 2011. **12**(1) DOI: 10.1186/1471-2105-12-124.
124. Buchfink, B., C. Xie, and D.H. Huson, *Fast and sensitive protein alignment using DIAMOND.* Nature Methods, 2014. **12**(1): p. 59-60 DOI: 10.1038/nmeth.3176.
125. Nierman, W.C., et al., *Genomic sequence of the pathogenic and allergenic filamentous fungus Aspergillus fumigatus.* Nature, 2005. **438**(7071): p. 1151-1156 DOI: 10.1038/nature04332.
126. Hubley, R., et al., *The Dfam database of repetitive DNA families.* Nucleic Acids Research, 2016. **44**(D1): p. D81-D89 DOI: 10.1093/nar/gkv1272.
127. Heng, L., *Aligning sequence reads, clone sequences and assembly contigs with BWA-MEM.* arXiv:1303.3997, 2013 DOI: https://doi.org/10.48550/arXiv.1303.3997.
128. Li, H., et al., *The Sequence Alignment/Map format and SAMtools.* Bioinformatics, 2009. **25**(16): p. 2078-2079 DOI: 10.1093/bioinformatics/btp352.
129. van Arkel, A.L.E., et al., *COVID-19–associated Pulmonary Aspergillosis.* American Journal of Respiratory and Critical Care Medicine, 2020. **202**(1): p. 132-135 DOI: 10.1164/rccm.202004-1038LE.
130. Danecek, P., et al., *The variant call format and VCFtools.* Bioinformatics, 2011. **27**(15): p. 2156-2158 DOI: 10.1093/bioinformatics/btr330.
131. Ortiz, E.M., *vcf2phylip v2.0: convert a VCF matrix into several matrix formats for phylogenetic analysis. (v2.0).* in *Zenodo*. 2019.
132. Stamatakis, A., *RAxML-VI-HPC: maximum likelihood-based phylogenetic analyses with thousands of taxa and mixed models.* Bioinformatics, 2006. **22**(21): p. 2688-2690 DOI: 10.1093/bioinformatics/btl446.
133. Ciccarelli, F.D., et al., *Toward Automatic Reconstruction of a Highly Resolved Tree of Life.* Science, 2006. **311**(5765): p. 1283-1287 DOI: 10.1126/science.1123061.
134. Supek, F., et al., *REVIGO Summarizes and Visualizes Long Lists of Gene Ontology Terms.* PLoS ONE, 2011. **6**(7) DOI: 10.1371/journal.pone.0021800.

## FIGURE CAPTIONS

**Figure 1. Certain *Aspergillus fumigatus* isolates display persistence to voriconazole.**

**A)** In disc-diffusion assays (10 µL of 0.8 mg/mL voriconazole), the susceptible isolate ATCC46645 never grew any colony in the inhibition halo, the resistant control (RC) isolate grew up to the edge of the disc. The strain PD-256 always grew numerous colonies that neatly covered the halo, and the persister isolate PD-104 was consistently able to grow a few small colonies. Plates were incubated for 5 days at 37°C. **B)** Inspection of the wells of a broth dilution assay under the microscope 72 hours after inoculation revealed that the non-persister isolates ATCC and PD-60 displayed only limited microscopic growth at the MIC concentration, and all conidia remained ungerminated at higher concentrations. In contrast, the persister strains PD-9 and PD-104 showed noticeable microscopic growth up to three fold (3x) the MIC concentration. Scale bar= 132.5 µm. **C)** Full content of the well containing the maximum concentration of voriconazole (8 µg/mL) was plated on rich media PDA plates and colony forming units (CFUs) counted 48 hours after inoculation. Persister isolates grew significantly more CFUs than non-persister isolates (PD-9 VS ATC46645C $p$=0.002 and PD-104 VS ATCC46645 $p$=0.0331), demonstrating that these strains remain viable upon azole treatment for a longer period. Three independent experiments with three biological replicates were performed, the graph represents the means and SD, and data was analysed using the Brown-Forsythe and Welch ANOVA test with Dunnett's multiple comparisons. **D)** A survival curve in the presence of 4 µg/mL of voriconazole revealed that, whilst non-persister strains lost viability very rapidly, the persister isolates had the characteristic bi-phasic reduction in viability, showing that a sub-population of the persister isolates remained viable for a longer period. The experiment was done in biological duplicates with two technical replicates, the graph represents the means and SD.

**Figure 2. *Aspergillus fumigatus* persistence does not depend on the morphological stage, but seems to be determined by the growth media**.

**A)** Conidia of the different isolates were inoculated and incubated for 8 or 16 hours before the disc containing voriconazole (10 µL of 0.8 mg/mL) was added to the RPMI plate. At 8 hours, when conidia have germinated, the persister isolates PD-9 and PD-104 were still able to grow small colonies in the inhibition halo, whilst the non-persister strains were not. At 16 hours, when conidia have already formed hyphae, the background growth made impossible to distinguish colonies in PD-9, but a clear one could be detected in PD-104. **B)** On *Aspergillus* minimal medium (MM), the persister isolate PD-104 was able to form colonies in the halo, but the non-persister strain ATCC was not. **C)** On rich media PDA and Sabouraud (Sab) all isolates were able to form conidia in the halo. **D)** This happened even the MIC of all isolates was the same in commonly assayed RPMI and the rich media Sab.

**Figure 3. *Aspergillus fumigatus* persistence is not influenced by stress, with the exception of hypoxia, and cannot be eliminated with adjuvant or combinatorial treatments.**

**A)** Hypoxia was the only stress that could prevent persistence, whilst neither oxidative ($H_2O_2$), cell wall (SDS or CFW) or osmotic (NaCl) stress influenced persistence. **B)** Hypoxia completely eradicated persistence also on the rich medium YAG for ATCC, PD-60 and PD-9, but only reduced persistence for the PD-104. **C)** The use of adjuvant drugs could not prevent persistence. **D)** Combinatorial treatment with amphotericin-B and caspofungin did not prevent persistence. All plates were incubated with 10 µL of 0.8 mg/mL voriconazole added to the disc and the specific condition (stress, adjuvant or combinatorial drug) as described in the text. Plates were incubated for 5 days at 37°C. All plates and conditions were repeated in two independent experiments.

**Figure 4. RNA-seq analysis reveals potential causes of persistence**.

**A)** Schematic representation of the conditions assayed, the comparisons made and the number of genes identified, as detailed in the text. In addition, the sites of sampling for the no drug (plate without voriconazole disc), low drug (light green circle at mid-distance of the inhibition halo) and persistence (colonies inside the inhibition halos) conditions are shown. **B-E** The most significantly upregulated GO biological processes are shown using the REVINGO tool for GO data visualization [134]. The full list of upregulated GO terms can be found in Tables S2-S5 and Table 2. **B**) PD-104 Persister only genes (aligned to the A1163 genome), **C)** all genes upregulated in Persistence (aligned to the pangenome), **D)** PD-104 Persister only genes, (aligned to the pangenome) and **E)** genes that are most upregulated in persistence compared to normal response to the drug.

**Figure 5. External addition of GAG potentiates persistence in the isolate PD-104**.

**A)** Addition of GAG does not change the MIC of the isolates. **B)** Representative merges of 87 photos to cover the whole well of broth dilution assays. The fungal material was stained with calcofluor white. Representative wells of PD-104 with and without GAG at 2X the MIC are shown **C)** Counting of germinated conidia/short hyphae in the entire wells of 2X (left) and 3X (right) MIC of broth dilution assays. External addition of GAG significantly increased the number of germlings in PD-104 from 1.09% to 2.80%, $p$=0.0267 at 2X MIC and from 0.41% to 0.75% $p$=0.038, two-tailed unpaired $t$-test. Two independent experiments with two technical replicates were performed. The graphs represent the means and SD. **D)** Plating of the entire content of wells containing 4 µg/mL of voriconazole shows that external addition of GAG significantly increased the number of viable PD-104 cells that can be recovered 48 hours after inoculation ($p$=0.0437, one way ANOVA with Tukey's multiple comparisons). Two independent experiments with three biological replicates were performed. The graph represents the means and SD.

**Figure 6. Persister isolates do not form a distinct lineage.**

The genomes of newly sequenced persister and non-persister isolates, as characterised in this study (Table S8), distributed scattered when included in the previously generated phylogenetic tree [62]. Therefore, persistence is not a feature that has evolved in a particular lineage.

**Figure 7. Voriconazole eliminates persister isolates less efficiently than non-persister strains in a *Galleria mellonella* infection model.**

**A)** Survival curve of larvae infected with $10^4$ conidia of the isolates ATCC, PD-60 (non-persisters), PD-9 or PD-104 (persisters). All strains killed larvae at a similar rate, demonstrating that they are equally virulent. Three independent experiments were done with 15-20 larvae/isolate in each. **B)** Fungal burden was measured by qPCR 72 h after infection with $10^4$ conidia. For all strains, fungal burden was greatly lower in larvae that had received a voriconazole treatment (8 µg/mL) that in those who had not. The reduction in burden was bigger in non-persister isolates than in persister isolates.

**Supplementary Figures**

**Fig. S1.**

Disc diffusion screening of the PD-47 collection of isolates (Table S1) on RPMI plate with 10 µL of 0.8 mg/mL voriconazole. Only 5 isolates could grow colonies in the inhibition halos. Upon re-inoculation of the colonies of the halo, PD-254, PD-256 and PD-266 covered the entire plate. As explained in the text those strains were classified as resistant or heteroresistant. In contrast, PD-9 and PD-104 CoHs showed upon re-inoculation the same level of growth as the original isolates. These strains were classified as persisters.

**Fig. S2.**

Disc diffusion screening of the PD-47 collection of isolates. Three days after inoculation, the disc containing voriconazole (10 µL of 0.8 mg/mL) was substituted for another one containing *Aspergillus* minimal medium. A few colonies were able to grow colonies in the halos after the switch, suggesting that a few conidia remain viable. Only three strains PD-9 and PD-104 and PD-259 grew colonies before the switch. Of those, only PD-9 and PD-104 grew additional colonies after the switch.

**Fig. S3.**

Independent repetitions of the experiment shown in Figure 1B. The wells of 1X, 2X and 3X MIC of voriconazole for the isolates ATCC, PD-9, PD-60 and PD-104 were imaged under the microscope. The non-persister isolates ATCC and PD-60 only displayed limited microscopic growth at 1X MIC. In

contrast, the persister isolates PD-9 and PD-104 displayed microscopic growth at 1X, 2X and 3X supra-MIC concentrations. Scale bar= 132.5 µm.

**Fig. S4**

Disc diffusion screening of the PD-47 collection of isolates (Table S1) on RPMI plate with 10 µL of 3.2 mg/mL itraconazole. Isolates RC (as expected) and PD-256 did not form an inhibition halo, reflecting that they are resistant to itraconazole. Isolates PD-104 and PD-266 could grow colonies in the halo. PD-104 formed upon re-inoculation a halo of the same size and similar number of CoHs as the original isolate, suggesting that it is persistence to itraconazole. The isolate PD-266 nearly covered the inhibition halo upon reinoculation, suggesting an increment in its MIC and therefore that it is likely heteroresistant to itraconazole, as previously described for voriconazole.

**Fig. S5**

**A)** MICs of itraconazole and isavuconazole for the isolates ATCC, PD-9, PD-60 and PD-104, as calculated by broth dilution assay. **B)** The isolates PD-9 and PD-104 displayed some microscopic growth at 2X the MIC concentration for both azoles, whilst the isolates ATCC and PD-60 did not grow at all and only resting conidia could be found. **C)** The entire content of the wells containing the highest concentration (8 µg/mL) if each azole were inoculated on PDA plates and incubated for 48 h at 37 °C. A noticeable ratio of viable conidia were detected for the isolates PD-9 and PD-104. Each experiment was repeated twice independently. The graph represents the means and SD

**Fig. S6.**

**A)** A nylon membrane was placed on the RPMI plate. Conidia were inoculated on the membrane and the disc containing voriconazole (10 µL of 0.8 mg/mL) was also put on it. As in a normal disc diffusion assay, an inhibition halo was formed, inside of which the persister strain PD-104 was able to grow small colonies, but the non-persister strain A1160 was not. **B)** A network of interacting proteins was detected by STRING ($p$=1.84e-08) when using as query the 64 genes upregulated only in persistence in PD-104. Seventeen proteins related with metabolism formed a node, formed a node suggesting a specific metabolic response during persister growth. **C)** Within the 18 genes that were upregulated in all comparisons, a tight node of 6 interacting proteins, related with ergosterol production, was detected by STRING ($p$<1.0e-16).

**Fig. S7.**

**A)** Representative disc diffusion plates carried out with the collection of isolates from the TAU medical centre. Six isolates were able to form CoHs, which did upon reinoculation form halos of the same size (MIC did not increase) and create a similar number of CoHs. **B)** Resazurin was added to the

broth dilution RPMI plate at a 0.002% (w/v) final concentration. The plate was incubated for 24 hours in a Tecan Infinity M-Plex plate reader and fluorescence was measured every 30 minutes with an excitation wavelength of 544 nm and reading emission at 590 nm using the i-control 2.0 software. The read for each well at each time point was normalize as follows: (read well time X– read 8 µg/mL voriconazole time X)/read well at time 0. The time point with the best dynamic range of values in the 1X, 2X and 3X MIC was found to be 20 hours, which was selected to determine the metabolic activity. A value of 0.1 was assigned as background and values above 1 were detected in sub-MIC (macroscopic growth). At 1X MIC, a slight metabolic activity could be detected for both the non-persister ATCC and the persister isolates PD-9 and PD-104. At 2X and 3X the MIC, slight metabolic activity could only be detected for the persister isolates. The experiment was performed once with two biological replicates, the graph represent the means and SEM.

**Supplementary Files**

**Table S1:** Collection of isolates used in this study.

**Table S2**: GO enrichment of genes regulated exclusively in Persistence (A1163 genome as reference).

**Table S3:** GO enrichment of genes regulated in Persiter VS Low Drug (Pangenome as reference).

**Table S4:** GO enrichment of genes regulated exclusively in Persistence (Pangenome as reference).

**Table S5:** Proteins included in the STRING network (genes upregulated only in Persistence).

**Table S6**: GO enrichment of genes regulated more in Persistence (Pangenome as reference).

**Table S7:** Proteins included in the STRING network (genes upregulated more in Persistence).

**Table S8:** List of environmental isolates in the UK collection. Identity of the sequenced genomes. List of the clinical isolates of the TAU collection.

**Table S9:** Example of the Quast obtained to determine the quality of the assembly, using the PD-104 genome.

**DataSet1:** RNA-seq results and analysis of the A1160 isolate grown in NoDrug and Low Drug.

**DataSet2:** RNA-seq results and analysis of the PD-104 isolate grown in NoDrug, Low Drug and Persister, using the A1163 genome as reference for the alignment of reads.

**DataSet3:** RNA-seq results and analysis of the PD-104 isolate grown in NoDrug, Low Drug and Persister, using the pangenome genome as reference for the alignment of reads.

**Video S1:** The persister isolate PD-9 pre-incubated in voriconazole resumes growth when the drug is withdrawn.

**Video S2** The persister isolate PD-104 pre-incubated in voriconazole resumes growth when the drug is withdrawn.

**Video S3** The non-persister isolate ATCC46645 pre-incubated in voriconazole resumes growth when the drug is withdrawn.

Fig. 1

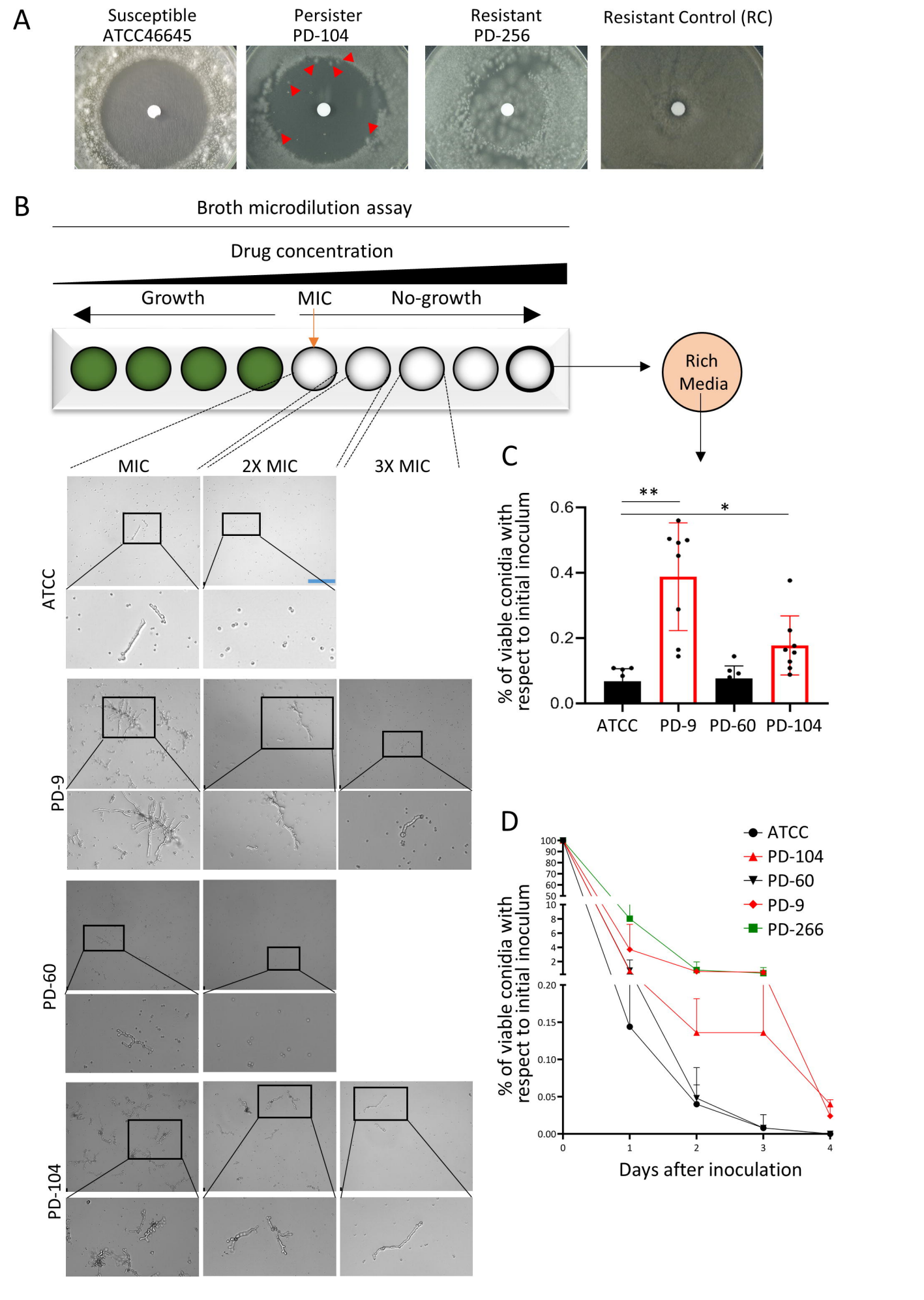

Fig. 2

A

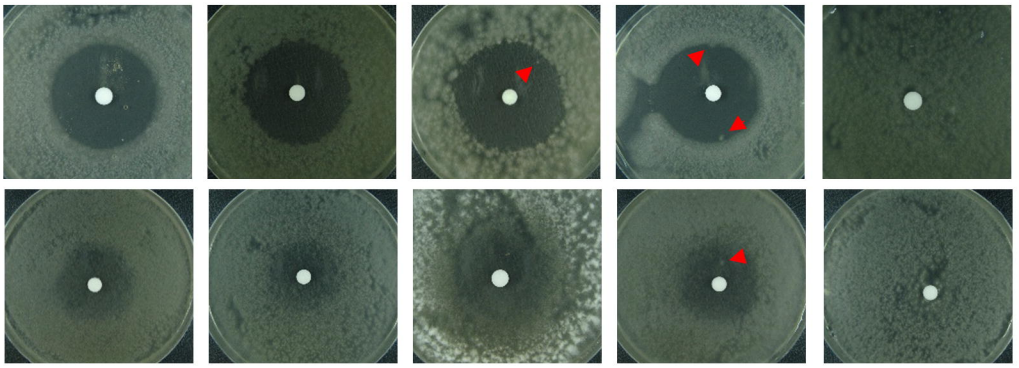


B

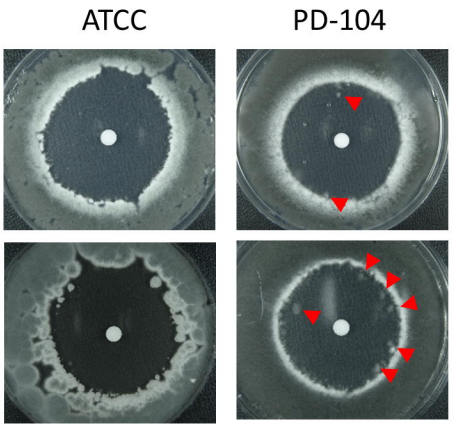


D

| Voriconazole | | |
|---|---|---|
| Isolate | MIC in RPMI | MIC in Sabouraud |
| ATCC | 0.25 | 0.25 |
| CEA10 | 0.25 | 0.25 |
| PD-9 | 0.5 | 0.5 |
| PD-104 | 1 | 1 |
| PD-60 | 1 | 1 |
| PD-266 | 8 | 8 |

C

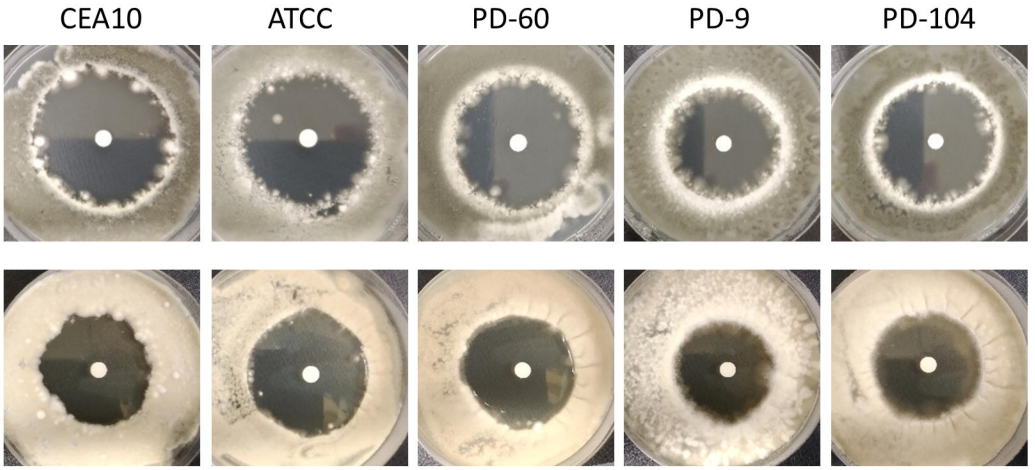

Fig. 3

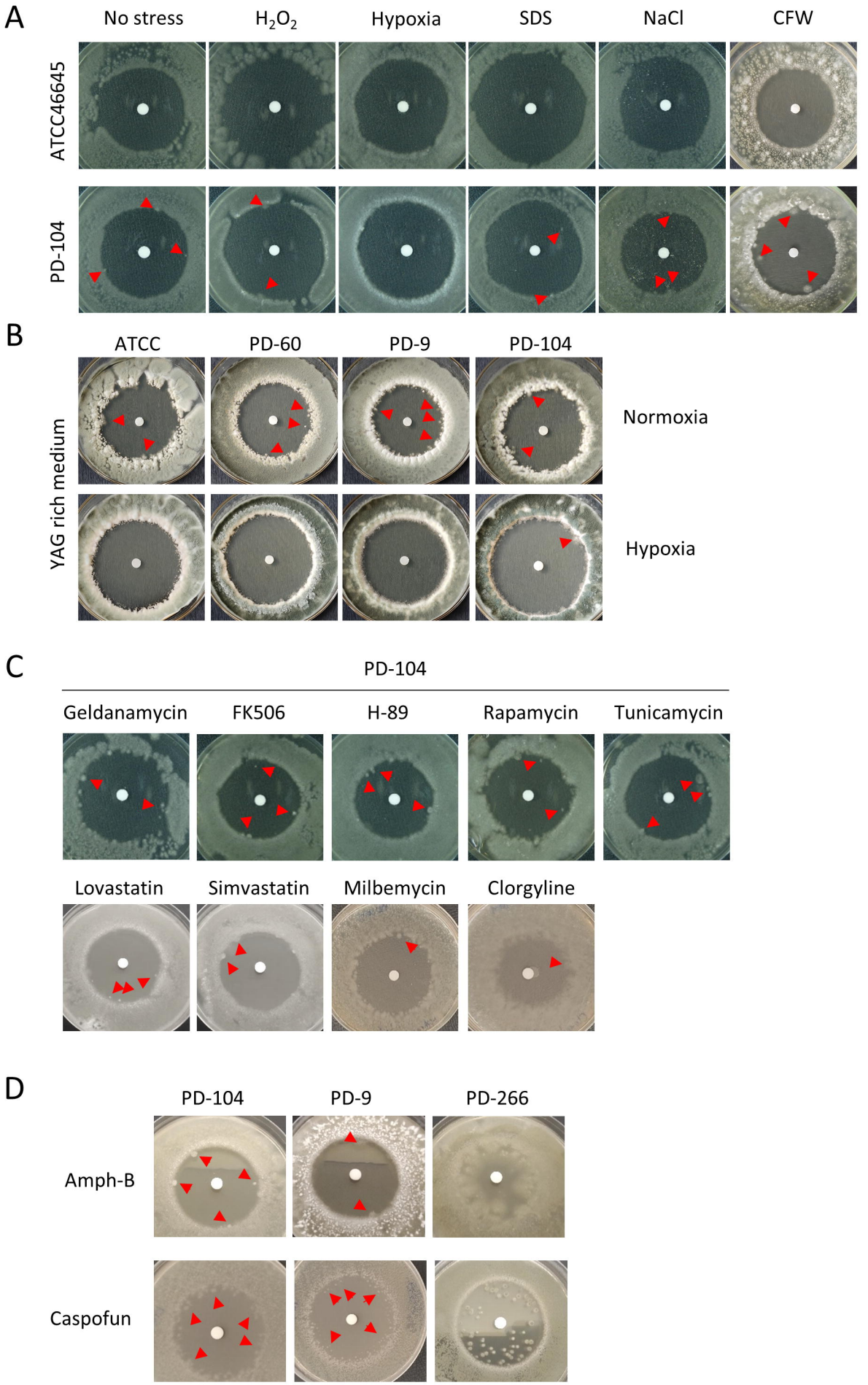

Fig. 4

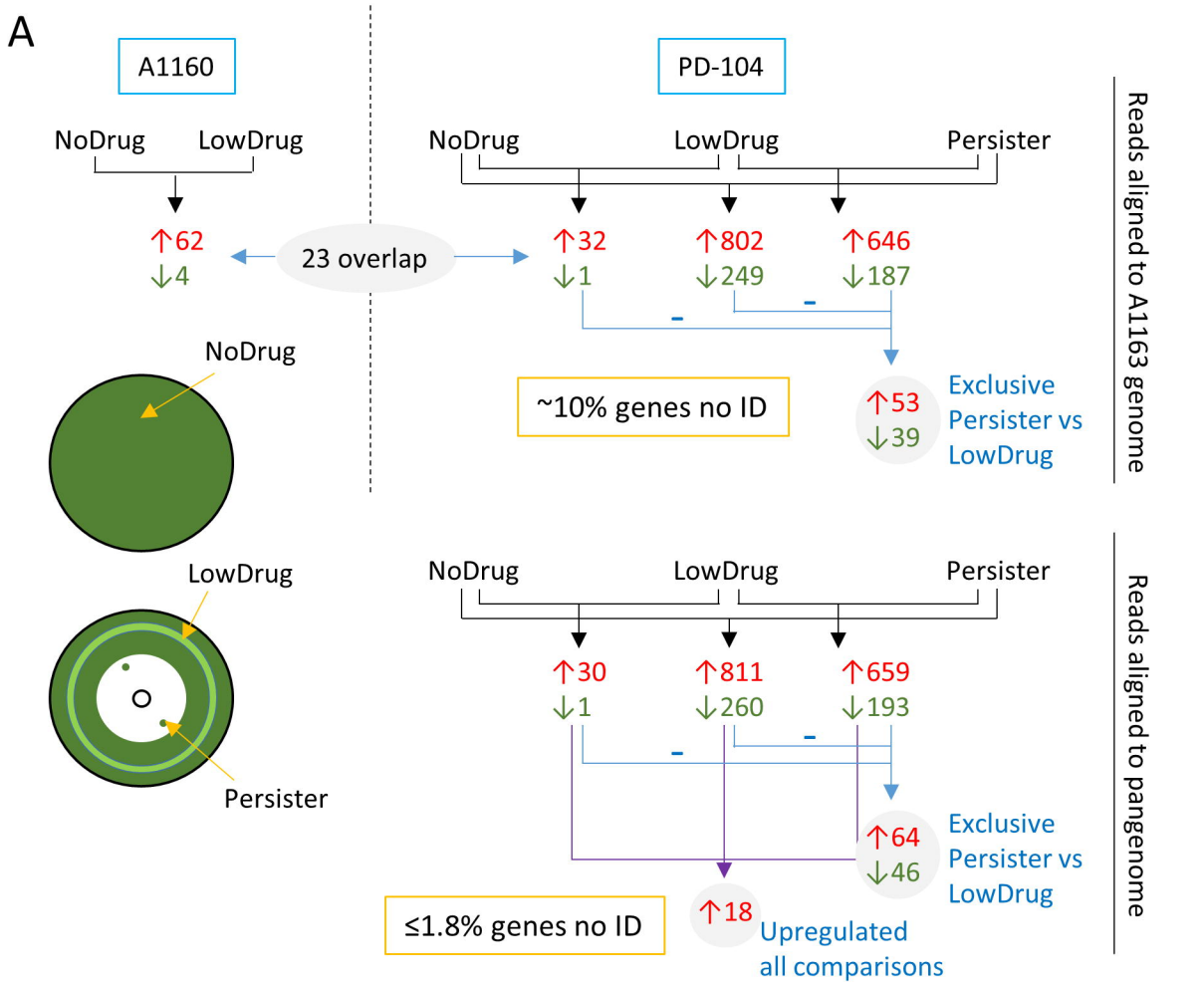


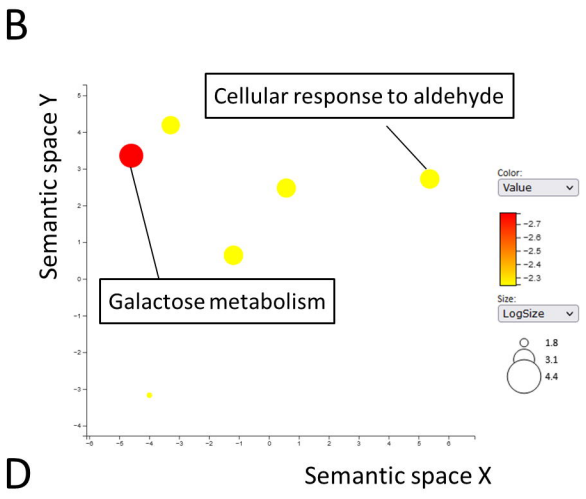


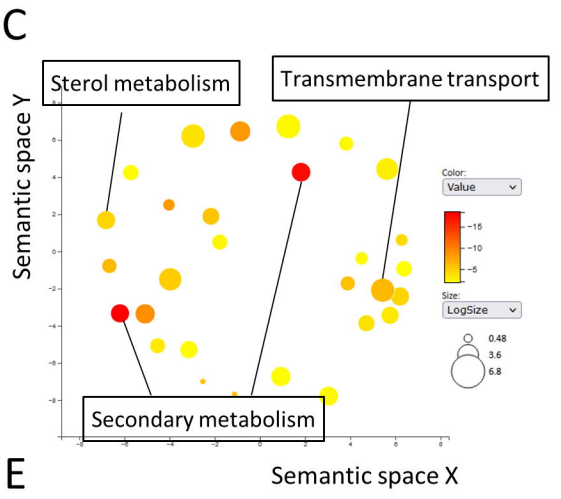


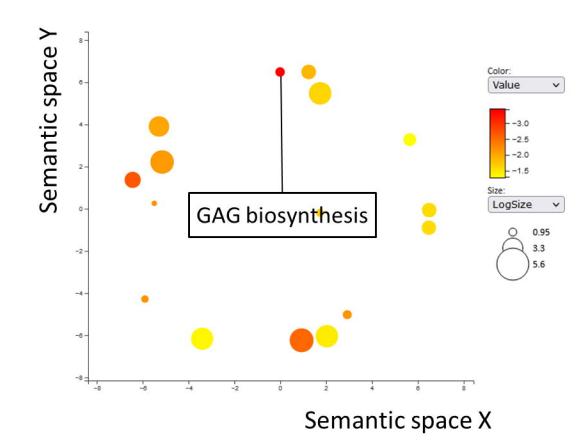


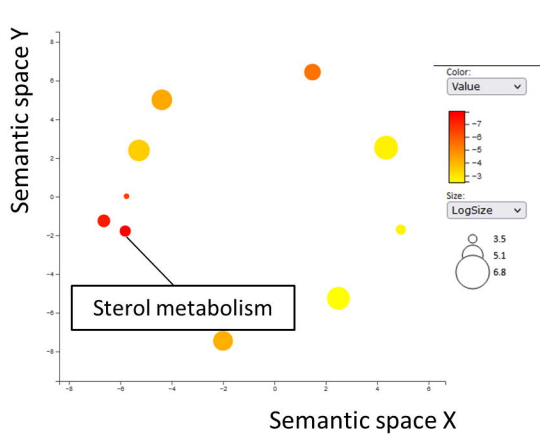

Fig. 5

A

| Voriconazole | | |
|---|---|---|
| Isolate | MIC | MIC +GAG |
| ATCC | 0.5-1 | 0.5-1 |
| PD-9 | 0.5-1 | 0.5-1 |
| PD-104 | 0.5-1 | 0.5-1 |
| PD-60 | 0.5-1 | 0.5-1 |

B

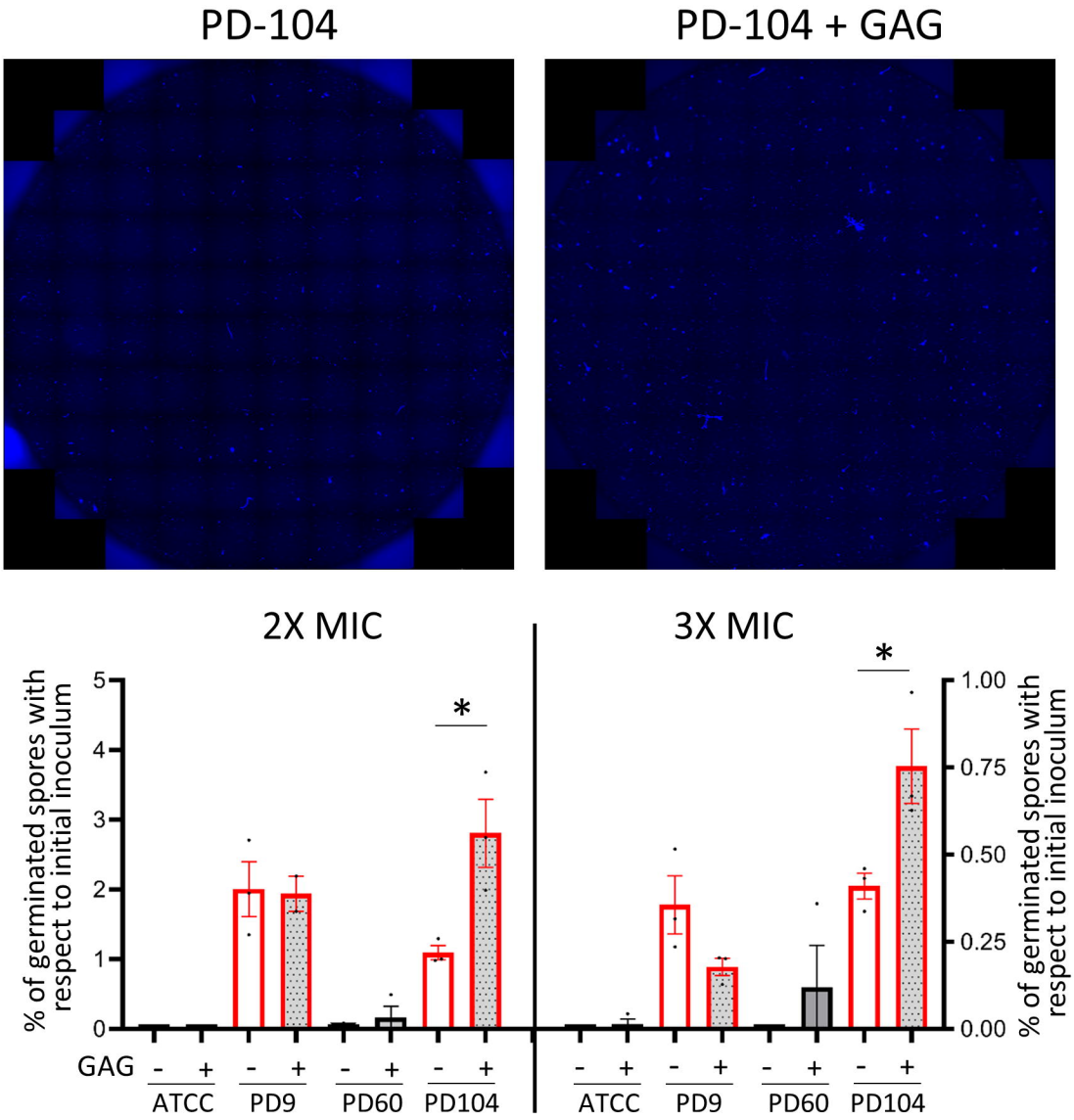


C

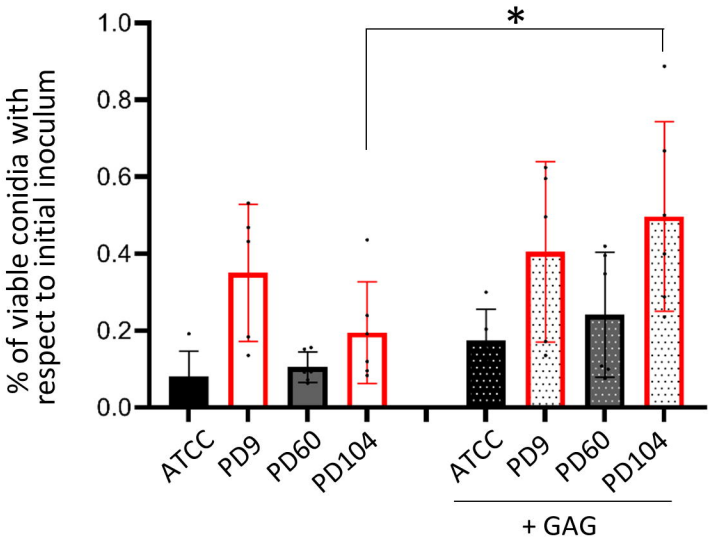

Fig. 6

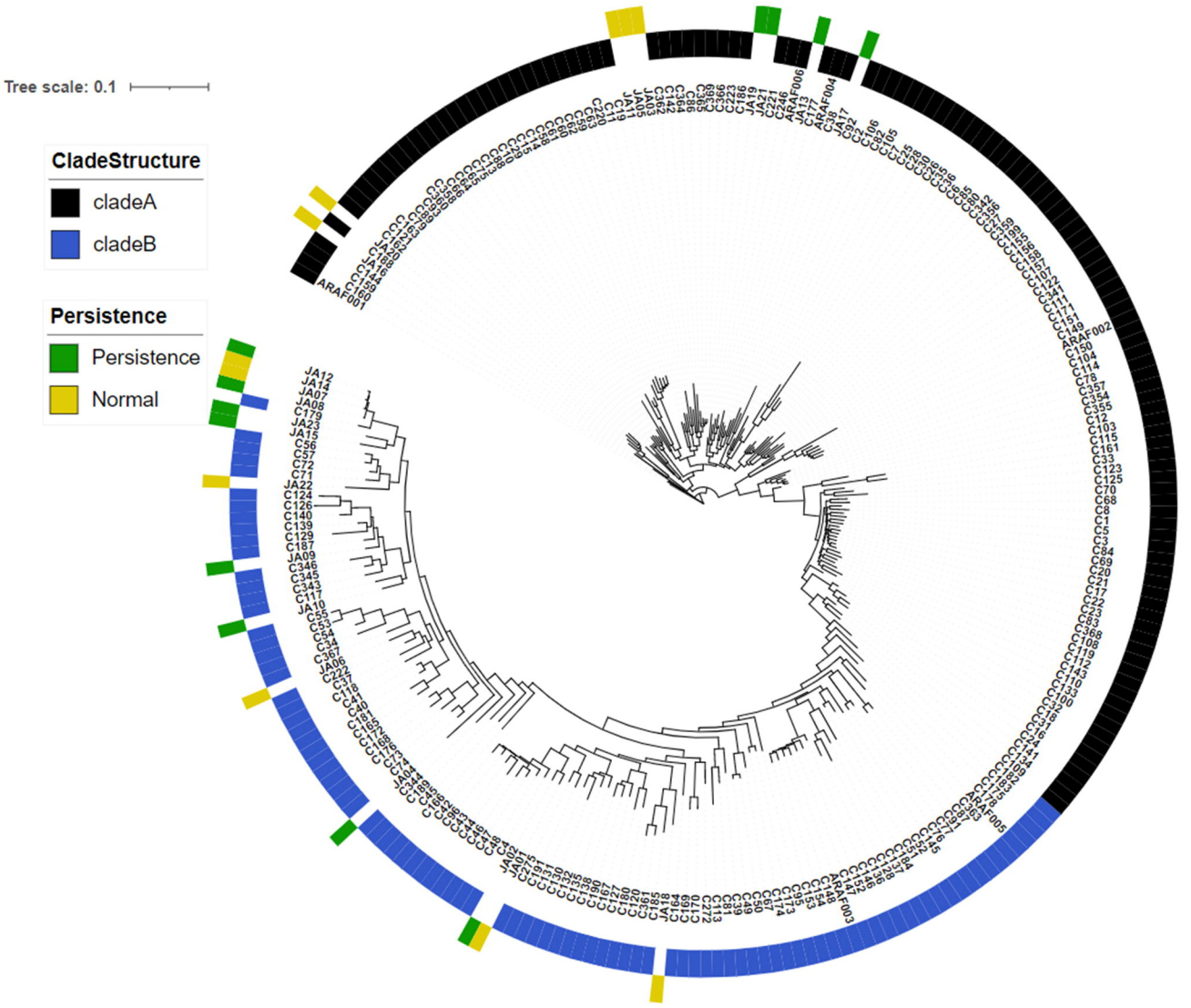

Fig. 7